AD-A149 579 STRENGTH AND STIFFNESS ANALYSIS OF NOTCHED GREEN OAK PALLET STRINGERS(U) FOREST PRODUCTS LAB MADISON WI T D GERHARDT DEC 84 FSRN-FPL-452 1/1

UNCLASSIFIED F/G 11/12 NL

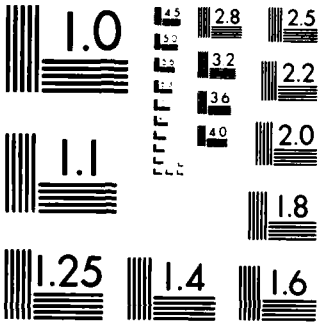

United States
Department of
Agriculture

Forest Service

Forest
Products
Laboratory

Research
Paper
FPL 452

Strength and Stiffness Analysis of Notched, Green Oak Pallet Stringers

Terry D. Gerhardt

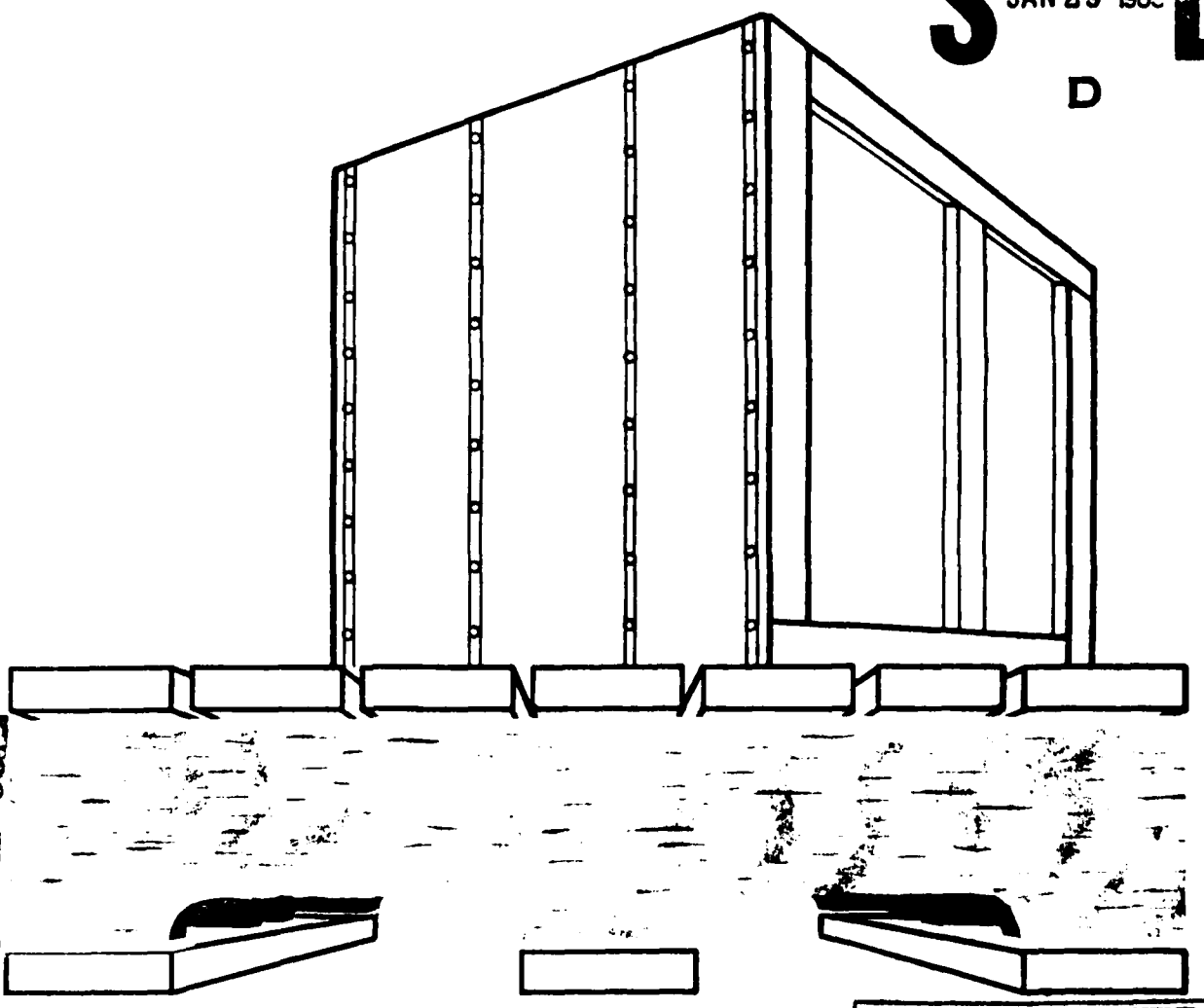

Abstract

Although 5.4 billion board feet of lumber was converted to 258 million pallets in 1980, design information for notched pallet stringers is limited. In this report, methodology is developed that determines stiffness and strength reductions caused by notches in pallet stringers.

A finite element (FE) structural model is developed to model notched stringers. Displacement and stress predictions agree well with experimental measurements. The author derived closed form equations that approximate FE displacements and maximum stresses as functions of notch depth. The stiffness equations are based on modeling the stringer with beam elements of an 'equivalent' geometry.

The stiffnesses and strengths of 600 full-size, green oak, pallet stringers with various notch geometries and loading conditions were measured. Measured deflections agreed well with stiffness equation predictions. Stringer strength was unaffected by varying the fillet radii of the notch from 1/2 inch to 1 inch. A group of stringers with sharp, rectangular notches (no fillet) had lower strength values than the filleted groups.

I derived equation (15) from the FE results to predict strength as a function of notch depth for any loading condition. By adjusting the equation, both mean and fifth percentile strengths were predicted. Agreement between predicted strengths and experimental results was excellent.

Keywords: Notched pallet stringers, notched beams, red oak, structural model, finite element model, stiffness, stress, fillet radii, filleted notches.

Acknowledgments

The author thanks Tom Foley of Foley and Sons, Bargersville, Ind., for donating the oak stringers used in this study. Also appreciated was the use of a notcher made available by Hazelthorn Machine Co., Terre Haute, Ind. The efforts of William Baldwin, executive vice president of NWPCA, in coordinating these donations are gratefully acknowledged.

The statistical design and analysis were capably handled by James Evans and Carol Link of Forest Products Laboratory (FPL). The author also acknowledges the support of Lisa Marin who helped formulate the study plan while employed at FPL.

December 1984

Gerhardt, T. D. Strength and stiffness analysis of notched, green oak pallet stringers. Res. Pap. FPL 452. Madison, WI: U.S. Department of Agriculture, Forest Service, Forest Products Laboratory; 1984. 25 p.

A limited number of free copies of this publication are available to the public from the Forest Products Laboratory, P.O. Box 5130, Madison, WI 53705. Laboratory publications are sent to over 1,000 libraries in the United States and elsewhere.

The Laboratory is maintained in cooperation with the University of Wisconsin.

Contents

Strength and Stiffness Analysis of Notched, Green Oak Pallet Stringers

Terry D. Gerhardt, Research Engineer
Forest Products Laboratory, Madison, Wis.

Introduction

Although 5.4 billion board feet of lumber were converted to 258 million pallets in 1980 (McKeever and Hatfield 1984), design information for notched pallet stringers is limited. Pallet design procedures as proposed by Wallin et al. (1976) consider design criteria for both stiffness and strength of notched stringer members. The deflection equations recommended are the standard elementary beam equations (uniform-unnotched beam, isotropic material, Bernoulli-Euler assumption, etc.) which are modified through an assumption that the deflection increase from notching is proportional to the material removed. The strength equations were also determined from beam theory without any real consideration of the stress concentration from the notch.

In this study, methodology is developed to systematically determine stiffness and strength reductions caused by notches in pallet stringers. The particular objectives are to:

(1) Determine the effects of varying notch depth and fillet radius on the strength and stiffness of oak stringers containing a single notch; and
(2) Develop design equations for conventional double-notched oak pallet stringers.

The scope of this study is limited to the short-term strength of green oak stringers. This study is part of a cooperative pallet research program involving the National Wooden Pallet and Container Association (NWPCA), Virginia Polytechnic Institute and State University (VPI&SU), and the Forest Service. Results from the study will be implemented in a computer structural model of a pallet, which is a main objective of the overall cooperative research program.

The notched beam literature has focused mainly on notches with sharp corners cut in clear wood. Hirai and Sawada (1980) present experimental results from tests on Akaezomatsu *(Picea glehnii)* with rectangular edge notches of various depths and widths. A size effect for both beam depth and width was observed, although the latter was not evident for beams with wide notches. An empirical model to predict moment-carrying capacity was derived based on the principles of linear elastic fracture mechanics (LEFM). Murphy (1979) also used a fracture mechanics approach to predict failing loads for slit-notched beams. Experimental results for clear Douglas-fir beams with both rectangular and slit notches are presented. Murphy concludes that slit-notched beams have a lower strength than rectangular-notched beams when the remainder of the geometry is the same. Stieda (1966) tested green and kiln-dried notched Western hemlock, Balsam fir, and Eastern white cedar. Results show that narrow notches have a relatively larger effect on strength than wide notches. Additionally, Stieda compares a small slit to a small semicircular hole and finds no great difference in strength.

Palka and Holmes (1973) report experimental results for small square-notch cantilever beams of green, clear Douglas-fir. Strength and stiffness versus depth regression equations were developed from the data. Ultimate loads and stiffnesses were found to strongly depend on beam depth. The strong dependence of strength on grain slope was observed by Leicester (1974) in tests of Australian timbers with sharp rectangular notches. The author also tested wood with slits of varying notch radii. Strength was found to be somewhat independent of notch root radii. Recently, Leicester and Poynter (1980) proposed design equations for beams with unfilleted notches. Richards (1974) tested clear, yellow-poplar beams with shallow, curved notches on the compression side. Richards found little dependence of strength on notch root radii or notch depth.

The notches cut in pallet stringers are rectangular edge notches with fillets for stress relief. Examination of the stiffness- and strength-reducing effect of this notch in wood beams has received limited attention in the literature. Stern (1972) tested pallet stringers to examine potential strength improvement from the use of cross nails in the notch region. The effects of notch geometry on strength were not considered. Recently Bastendorff and Polensek (1981.1984) tested notched and unnotched red alder pallet stringers. The effects of notching on modulus of elasticity (MOE) and modulus of rupture (MOR) are presented for one particular geometry. The results indicate a 37-44 percent reduction in MOR for notches with a 9-inch width, 1.25-inch depth, and fillet radius of 0.75 inch.

Experimental Procedure

In this section, experimental procedures are detailed. In summary, 600 oak pallet stringers were selected from a single mill using industry quality guidelines. Pallet-type notches of varying geometries were cut into 510 of the stringers. Boards were mechanically tested to examine effects of loading conditions and notch geometry on stiffness and strength of pallet stringers.

Materials

Red oak pallet stringers were selected from a single mill. Boards were green and had approximate dimensions of 48 x 3.75 x 1.5 inches. In selecting each board, NWPCA quality guidelines for pallet stringers (NWPCA 1982) were followed. Rules for both limitation of defects in the stringers and notch geometry are summarized below.

1. *Knots and holes.* The diameter of sound knots shall be no greater than one-half the width of the piece in which they occur. Loose or hollow knots and holes shall not exceed one-quarter the width of the piece in which they occur. Knots over 1/2 inch shall not be allowed in the stringer immediately over the notched areas.

2. *Splits, shakes, and checks.* Crack or grain separation length must be no longer than twice the width of the piece if contained by nailing. Checks are unlimited in quantity, length, and location.

3. *Cross grain.* Slope of grain must not exceed 1 inch in 5 inches.

4. *Wane.* Wane is limited in stringers to one-third nailing face, one-half other face, and unlimited in length.

5. *Decay.* Decay is not permitted.

6. *Notches.* To be 1-1/2 inches deep x 9 inches long across the bottom, 3/4-inch radial cuts at top corners, and a minimum 7-inch flat surface at the top. All dimensions excepting the minimum to be $\pm$ 1/4 inch.

These rules were amended slightly in regard to restriction of 1/2-inch knots near the notch. Typical specifications often require that no knot be within 2 inches of the cutout area (Mclain 1982). This criterion was used in the selection process.

Stringers were randomly sorted into nine different groups. Every group was associated with either a particular notch geometry (single or double) or an unnotched control group. The amended criteria for knots near the notches complicated the selection process. For each group, knots were excluded from different regions of the stringer depending on location and depth of the notch or notches to be cut. The knot criteria, in effect, sorted stringers with various amounts of clear wood into different groups. Generally speaking, an increasing amount of clear wood was contained in groups with stringers that were:

(1) unnotched,
(2) single notched, and
(3) double notched.

Boards not satisfying knot or other grading requirements for the group being sought were rejected. A total of 1,480 boards were sampled to obtain the 600 selected.

Methods

After sampling was completed, 1 or 2 notches were cut in 390 boards with an industrial (single) notching machine. Two notches were cut by making two passes on the same stringer. Details of the various notch geometries cut are described in the next section. After notching, all 600 boards were dipped in a 0.5 percent solution of *sodium pentachlorophenate* to inhibit the growth of blue stain. The boards were then stacked for several minutes before being loaded on pallets and sealed in plastic. The stringers were transported to the Forest Products Laboratory (FPL), Madison, Wis., and stored at 36° F until tested mechanically. In this manner, boards were maintained in green condition.

Experimental Design

The 9 groups based on notch geometry were randomly subdivided into 20 groups containing 30 boards each. Each of the 20 groups represents a specific notch geometry and loading condition. The groups all fit into one of the following categories:

(1) stringers containing a single center notch (fig. 1),
(2) stringers containing two notches cut symmetrically about the center of the stringer (fig. 2), and
(3) unnotched stringers.

Figures 1 and 2 give the geometric quantities defining board and notch dimensions which are: stringer length (ℓ), stringer height (h), stringer thickness (t), notch depth (D), notch width (W), fillet radius (ρ), and distance between notches (2q) (fig. 2 only). The geometric quantities defining load and support conditions are: distance between supports or span (s), distance between support and symmetric load point (a), and distance between support and closest notch edge (m).

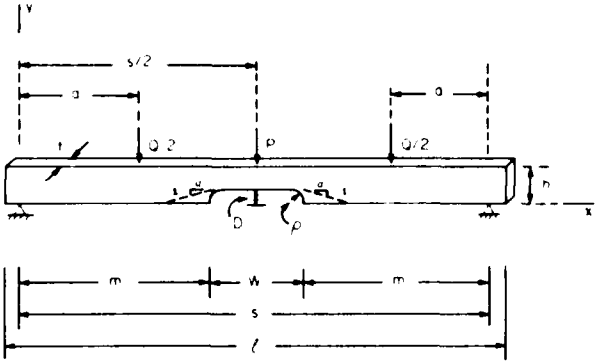

Figure 1.—Single-notched stringer geometry. (ML84 5507)

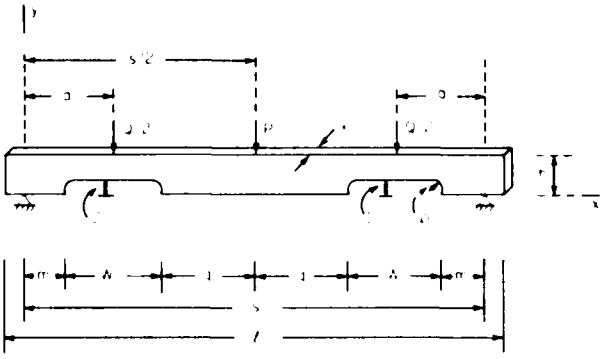

Figure 2.—Double-notched stringer geometry. (ML84 5505)

The following scheme was used for the group identification labels. The first letter refers to loading condition: M and C indicate two-point and center-point loading, respectively. For groups containing single notched stringers, the second letter refers to a particular notch dimension which is varied in a series of groups. Thus, the letters D, R, and S indicate notch depth, fillet radius, and cut slit at fillet, respectively. For groups containing stringers which are double-notched or unnotched the second letter is T or C respectively.

Single-Notched Stringers

Although pallet stringers are double notched, single, center-notched stringers (fig. 1) more clearly expose the effects of notch depth, fillet radius, and loading conditions on stiffness and strength. Notch dimensions and loading conditions for the groups containing single, center notches are presented in table 1. All boards have common dimensions: W = 9.0 inches, s = 44 inches, and m = 17.5 inches.

Table 1.—Groups containing single-notched stringers[1] (fig. 1)

Group identification	Boards tested	Loading	Notch dimensions	
			ρ	D
			In.	
M-D-1	30	QP[2]	0.50	1.0
M-D-2	30	QP	.50	1.5
M-D-3	[3]29	QP	.50	1.875
M-D-4	30	QP	.50	2.5
C-D-1	30	CP[4]	.50	1.0
C-D-2	30	CP	.50	1.5
C-D-3	30	CP	.50	1.875
C-D-4	[3]28	CP	.50	2.5
M-R-1[5]	30	QP	.50	1.5
M-R-2[5]	30	QP	.75	1.5
M-R-3[5]	30	QP	1.00	1.5
M-R-0[5]	30	QP	([6])	1.5
M-S-1[7]	30	QP	.50	1.5
M-S-2[8]	30	QP	.50	1.5

[1] Stringer dimensions (approximate): ℓ = 48 in., h = 3.75 in., and t = 1.5 in. Notch and support dimensions: W = 9.0 in., s = 44 in., and m = 17.5 in. (see fig. 1).

[2] Quarter-point loading (a = 11 in.).

[3] Mistakes during notching resulted in less than 30 boards.

[4] Center-point loading.

[5] Notches cut at FPL.

[6] Sharp notch, no fillet.

[7] 1/2-in. slit cut into top of fillet.

[8] 3-in. slit cut into top of fillet.

In series M-D-1 through M-D-4 and series C-D-1 through C-D-4 the effect of notch depth on stringer stiffness and strength is examined under quarter point (a = 11 in.) and center-point loadings, respectively. The industrial notcher was adjusted to cut notch depths varying from 1.0 to 2.5 inches (see table 1). The notcher cut an approximate fillet radius of ρ = 0.50 inch. This radius represents the low end of the NWPCA allowable (0.75 in. ± 0.25 in.).

The effect of fillet radius on stringer stiffness and strength was examined with groups M-R-1 (ρ = 0.50 in.), M-R-2 (ρ = 0.75 in.), M-R-3 (ρ = 1.00 in.), and M-R-0 (sharp notch). All four groups were quarter-point loaded and had notch depths of D = 1.5 inches. Since the fillet radii were not readily changeable on the industrial notcher, the notches were cut at FPL. The procedure followed was to drill appropriate size holes in the stringer and then cut the remainder of the notch with a bandsaw. The industrial notcher utilized cutting tools mounted on a rotating shaft. Comparison of results from groups M-D-2 and M-R-1 allows a comparison of the notching techniques; stringers in the two groups have the same notch geometry and loading conditions.

Two additional groups (M-S-1 and M-S-2) had stringers notched on the industrial notcher with D = 1.5 inches and ρ = 0.50 inch. Stringers in these groups had slits cut parallel to the wood grain at the top of the fillet with a bandsaw. The slits were cut at FPL and were either 1/2 inch (M-S-1) or 3 inches (M-S-2) in length. These groups allow a qualitative examination of the effect of splits at the fillet on stringer stiffness and strength.

Double-Notched Stringers

The experimental design of the three groups containing double-notched stringers (fig. 2) is presented in table 2. All boards had common dimensions: D = 1.5 inches, W = 9 inches, ρ = 0.50 inch, and q = 8.5 inches. Groups C-T-1 and C-T-2 were center-point loaded, and group M-T-1 was two-point loaded (a = 9.0 in.). The spans were s = 44 inches (m = 4.5 in.) for groups C-T-1 and M-T-1 and s = 40 inches (m = 2.5 in.) for group C-T-2. The two spans examine the effects of support length on stringer stiffness and strength.

Unnotched Stringers

Unnotched stringers were tested in quarter-point (M-C-1) and center-point (C-C-1 and C-C-2) loadings as shown in table 3. Spans were s = 44 inches for groups M-C-1 and C-C-1 and s = 40 inches for group C-C-2.

Table 2.—Groups containing double-notched stringers[1] (fig. 2)

Group identification	Boards tested	Loading	Notch dimensions	
			s	m
			In.	
M-T-1	30	TP[2]	44	4.5
C-T-1	30	CP[3]	44	4.5
C-T-2	30	CP	40	2.5

[1] Stringer dimensions (approximate): ℓ = 48 in., h = 3.75 in., and t = 1.5 in. Notch and support dimensions: D = 1.50 in., W = 9.0 in., ρ = 0.50 in., and q = 8.5 in. (see fig. 2).

[2] Two-point loading, a = 9.0 in.

[3] Center-point loading.

Table 3.—Groups containing unnotched stringers[1]

Group identification	Boards tested	Loading	s
			In.
M-C-1	30	QP[2]	44
C-C-1	30	CP[3]	44
C-C-2	30	CP	40

[1] Stringer dimensions (approximate): ℓ = 48 in., h = 3.75 in., and t = 1.5 in.

[2] Quarter-point loading, a = 11 in.

[3] Center-point loading.

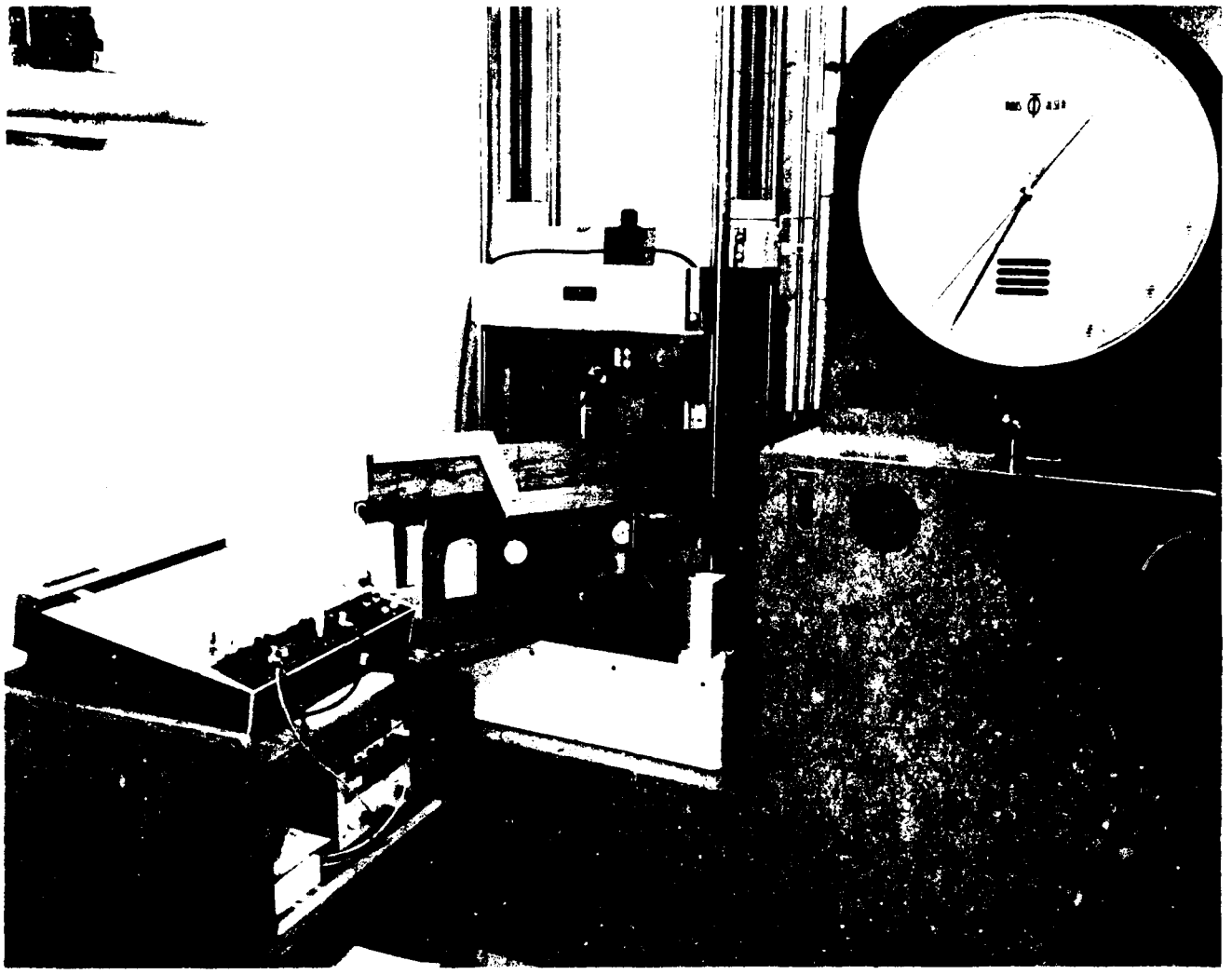

Test Procedures

[illegible] was loaded on a constant deflection [illegible] machine at a deflection rate set so [illegible] approximately 10-15 minutes. The test [illegible] equipment are shown in figure 3.

[illegible] was measured by initially loading the [illegible] between 100-500 pounds depending on notch depth. For each board, deflections were measured at [illegible] (see figs. 1 and 2) on the bottom [illegible] surface using dial gages. Stringers were then [illegible] and reloaded until failure. A linear-variable-differential transducer (LVDT) monitored deflection at [illegible] until failure. This midspan deflection was measured at mid-depth, that is, at (h-D)/2 for single-notched stringers. Plots of load versus deflection were recorded for each stringer and used to determine ultimate load. For the notched stringers, the plot also determined the load at which the crack initiated at the fillet.

After failure, specimens were cut near the fillet to determine approximate stringer moisture content and specific gravity.

Theory

Finite element (FE) structural models of notched pallet stringers are presented in this section. Displacements and fillet stresses are computed for various notch geometries and stringer material properties. Closed form equations for stiffness and maximum fillet stress are also derived.

Finite Element Modeling

FE models of double- and single-notched stringers are shown in figures 4 and 5, respectively. Note the exploitation of symmetry in the modeling. Cubic isoparametric plane elements (Zienkiewicz 1977) model the stringer except in the vicinity of the fillet. The 12-node isoparametric elements are contained in a computer program developed by the author (Gerhardt 1983).

The fillet region of the notched stringer is modeled with a special hybrid FE (Gerhardt 1984). Formulation of this element contains the following features:

(1) All governing differential equations of linear elasticity theory are satisfied in the element's interior using complex variable theory.

(2) The shape and stress-free conditions are satisfied exactly on the fillet surface using conformal mapping and reflection arguments.

(3) Continuity of analytic and polynomial displacement fields is satisfied in an approximate manner on the remaining boundary using a variational principle.

Results employing a hybrid element with conventional displacement-based finite elements were compared previously with elasticity solutions (Gerhardt 1984). The hybrid element was found to be remarkably accurate and efficient.

The author's computer program generates meshes from specification of h, D, ρ, and Ω. Variable Ω is defined as the lengths of the two sides of the hybrid element closest to the fillet as shown in figures 4 and 5. Modeling with the hybrid element is convenient since accurate results are obtained using a single element at each fillet. Further, the cubic element computes fairly consistent results, even as its aspect ratio is changed when meshes with different notch geometries are generated.

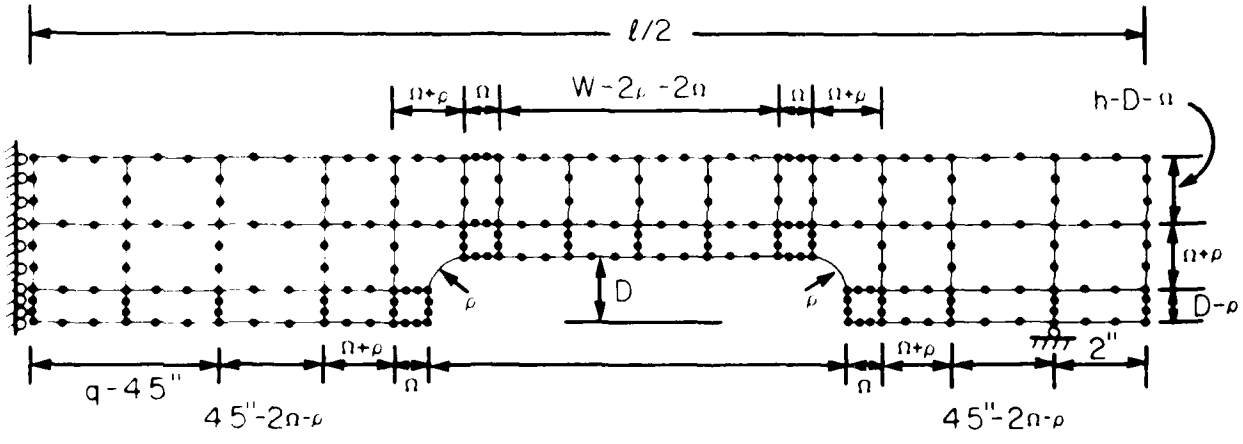

Figure 4 –FE mesh for double-notched stringers. (ML84 5509)

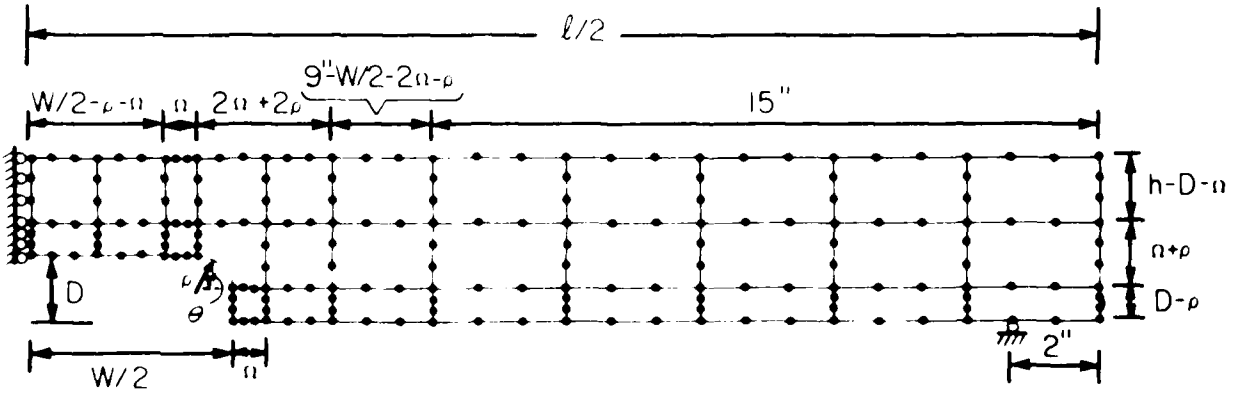

Figure 5 –FE mesh for single-notched stringers. (ML84 5510)

In Appendix A, FE computed displacements are compared to experimental measurements on a small, single-notched, Sitka spruce stringer. FE computed fillet stresses are compared to photoelasticity measurements. These comparisons with experimental data indicate that the FE model computes reliable displacements and fillet stresses.

Assumed Elastic Properties

For an orthotropic solid loaded in plane stress, the governing differential equation of linear elasticity theory can be formulated in terms of the material constants ϵ and κ (Gerhardt and Liu 1983) where

$$\epsilon = \sqrt[4]{\frac{E_x}{E_y}} \quad \text{and} \quad \kappa = \frac{1}{2\epsilon^2}\left(\frac{E_x}{G_{xy}} - 2\nu_{xy}\right) \qquad (1)$$

The constants E, G, and ν represent Young's modulus, the shear modulus, and Poisson's ratio, respectively. Subscripts indicate directions in the standard manner.

When the x direction is associated with the longitudinal (ℓ) axis and the y direction with the radial (r) or tangential (t) axes, the term $2\nu_{xy}$ is much smaller than E_x/G_{xy} for most wood species (Bodig and Goodman 1973). Thus, computed displacements and stresses can depend on the value chosen for ν_{xy} only slightly. Furthermore, the results can be characterized in terms of the ratios $E_\ell/G_{\ell y}$ and E_ℓ/E_y.[1] The ratios chosen for the FE analysis which follows are listed in table 4. Most wood species have elastic property ratios that fall between these broad ranges (Bodig and Goodman 1973). All FE calculations employed plane stress analysis with E_ℓ = 1,500,000 lb/in.^{2} and ν_{xy} = 0.35.

Stiffness

The accuracy of the FE model is experimentally verified in Appendix A for stiffness computations. Closed form equations, however, are preferred for design applications. Further, the FE stringer models cannot be readily used in a structural pallet model. Using such a detailed model for each stringer will result in an excessive number of degrees of freedom for the pallet.

In this section, closed form equations for stringer stiffness are derived. These equations are based on a simplified structural model for a notched stringer. The closed form equations are compared to FE results.

[1] Displacement boundary conditions will introduce other combinations of elastic constants into the formulation (Gerhardt and Liu 1983). In modeling the stringers, the only displacement conditions imposed are at the supports. Any difference in stress computation between this problem and one with the resultant forces applied at the supports must be localized in nature by Saint Venant's principle (Timoshenko and Goodier 1970).

Table 4.—Assumed elastic property ratios for FE analysis[1]

Group identification	$E_\ell/G_{\ell y}$	E_ℓ/E_y
G8-E6	8	6
G8-E12	8	12
G16-E12	16	12
G16-E24	16	24
G32-E12	32	12
G32-E24	32	24

[1] E_ℓ = 1,500,000 lb/in.^{2} and $\nu_{\ell y}$ = 0.35 for all.

Stiffness Equations

Hirai and Sawada (1979a) developed a method for estimating center deflection in wood beams containing square notches. The method is loosely based on the concept of released strain energy. In essence, the notch is replaced by tapered and rectangular sections as indicated by dashed lines in figure 1. The slopes of the tapered sections are specified by the constant α as shown. The authors computed center beam deflection for this 'equivalent' geometry using elementary beam theory. They empirically determined α from third-point bending tests of one species (*Abies sachalinenis* Mast.) with beams of dimension s = 750 mm, h = 50 mm, and t = 20 mm, and a center notch of width W = 10 mm (see fig. 1) for the cases ϕ = 0.10, 0.30, and 0.50, where ϕ is defined as the dimensionless notch depth, $\phi = D/h$. The best experimental-theoretical agreement was obtained by taking α = 5. The authors also tested additional beams with notch dimensions ranging from W = 3 to 80 mm and ϕ from 0.10 to 0.50. Center deflections computed by the model with α = 5 agreed well with experimental measurements. In another study Hirai and Sawada (1979b) tested beams of seven different Japanese wood species with notches of various depths and saw kerf width (3.0 mm). Good experimental-theoretical (α = 5) agreement was obtained for both center-point and third-point loading.

Differences in deflections of wood beams containing square notches compared to filleted notches will be negligible. The method previously described is therefore applicable for notched pallet stringers. One modification was made in derivation of equations presented here. Hirai and Sawada (1979b) replaced the distance between double notches by a flat section of minimum width, i.e., h = D. Calculated deflections were larger than measured deflections by 2 to 33 percent. The difference may be even greater for pallet stringers due to the substantial distance between notches. In the equations derived here, 'equivalent' tapered sections are used on both sides of both notches.

Utilizing this 'equivalent' geometry, closed form expressions for deflection of any point can be derived using Castigliano's theorem (Seely and Smith 1955). Although the equivalent geometry is quite simple, algebraic manipulation becomes quite tedious. Computations were therefore done in symbolic algebra (Hearn 1973) on a Sperry 1100/82 computer. Stringer deflections δ_P (at x = s/2) and δ_Q (at x = a) were considered.

The author derived the following expressions for double-notched stringers (fig. 2) loaded under three different conditions: center point (CP), two point (TP), and uniform (U). For all cases, $m \leq a \leq m + W$.

$$\delta_P = \frac{Ps^3}{48EI}\psi_{1P} \qquad \text{CP load} \qquad (2a)$$

$$\delta_Q = \frac{Pa(3s^2 - 4a^2)}{48EI}\psi_{1Q} \qquad \text{CP load} \qquad (2b)$$

$$\delta_P = \frac{Qa(3s^2 - 4a^2)}{48EI}\psi_{2P} \qquad \text{TP load} \qquad (3a)$$

$$\delta_Q = \frac{4Qa^2(3s - 4a)}{48EI}\psi_{2Q} \qquad \text{TP load} \qquad (3b)$$

$$\delta_P = \frac{5ws^4}{384EI}\psi_{3P} \qquad \text{U load} \qquad (4a)$$

$$\delta_Q = \frac{wa(s^3 - 2sa^2 + a^3)}{24EI}\psi_{3Q} \qquad \text{U load} \qquad (4b)$$

The author also derived the following expressions for single-notched stringers (fig. 1). For all cases, $0 < a \leq m$ and $0 < m < \alpha D$.

$$\delta_P = \frac{Ps^3}{48EI}\eta_{1P} \qquad \text{CP load} \qquad (5a)$$

$$\delta_Q = \frac{Pa(3s^2 - 4a^2)}{48EI}\eta_{1Q} \qquad \text{CP load} \qquad (5b)$$

$$\delta_P = \frac{Qa(3s^2 - 4a^2)}{48EI}\eta_{2P} \qquad \text{TP load} \qquad (6a)$$

$$\delta_Q = \frac{4Qa^2(3s - 4a)}{48EI}\eta_{2Q} \qquad \text{TP load} \qquad (6b)$$

$$\delta_P = \frac{5ws^4}{384EI}\eta_{3P} \qquad \text{U load} \qquad (7a)$$

$$\delta_Q = \frac{wa(s^3 - 2sa^2 + a^3)}{24EI}\eta_{3Q} \qquad \text{U load} \qquad (7b)$$

The constants in these expressions are defined as follows:

(1) P and Q/2 are concentrated loads applied as shown in figures 1 and 2.
(2) w is a uniform, distributed load applied between the supports with dimension force-length.
(3) Dimensions s and a are defined in figures 1 and 2.
(4) E is the modulus of elasticity (MOE) and it contains shear deformation and depends on loading conditions.
(5) I is the second area moment for the unnotched cross section, i.e. $I = th^3/12$.
(6) ψ_{ij} and η_{ij} are dimensionless factors defined in Appendix B which depend only on geometrical quantities, i.e. on ϕ, m, h, W, a, s, and α.

The coefficients of ψ_{ij} and η_{ij} in each expression are unnotched beam deflections for the relevant location and loading condition. The factors ψ_{ij} and η_{ij} should be interpreted as the contribution of the notch to beam deflection.

Comparison of Stiffness Equations with FE Results

FE stringer models were generated with the same geometries as those mechanically tested. All models generated had dimensions: $\ell = 48$ inches, $h = 3.75$ inches, $t = 1.5$ inches, $s = 44$ inches, $W = 9.0$ inches, and $\rho = 0.5$ inch. For the double-notched stringers: $a = 9.0$ inches, $m = 4.5$ inches, and $q = 8.5$ inches. For the single-notched stringers: $a = 11.0$ inches and $m = 17.5$ inches. For these geometries, notch depth was varied in seven equal increments from $D = 1.0$ to 2.5 inches ($\phi = 0.267$ to 0.667). Models were generated for all six property sets of table 4. Deflections δ_P (at $x = s/2$) and δ_Q (at $x = a$) were computed at middepth of the stringer cross sections for center-point, two-point, and uniform loading.

Results indicated that doubling the ratio E_ℓ/E_y changed computed deflections by only 0.5 to 1.5 percent. This negligible variation of stringer stiffness with assumed E_ℓ/E_y ratio was observed for all three $E_\ell/G_{\ell y}$ ratios. Deflections were more sensitive to assumed $E_\ell/G_{\ell y}$ ratio. Computed deflections for group G32-E12 exceeded those of group G8-E12 by as much as 22 percent for the same notch depth.

Young's modulus (E_ℓ) and the shear modulus ($G_{\ell y}$) are required as input for the FE analysis, while MOE (E) is required in the stiffness equations. Relations between these quantities can be derived using beam theory. Shear deflections can be computed by Castigliano's Theorem (Seely and Smith 1955) or by a method developed by Orosz (1970). I derived the following relations:

$$E = \frac{E_\ell}{1 + \lambda \frac{E_\ell}{G_{\ell y}}} \qquad (8)$$

where $\lambda = 1.2\ h^2/s^2$ for center-point loading, $\lambda = 2.4\ h^2/(3s^2 - 4a^2)$ for two-point loading, and $\lambda = 0.96\ h^2/s^2$ for uniform loading.

From the FE results, the stiffness equations (2), (7), and (8), FE ψ_s and η_s values were computed for the three E_s/G_s ratios. In all, 126 coefficients were computed (7 notch depths x 3 property sets x 3 loading conditions x 2 deflection locations) for both single- and double-notched stringers. These were compared to ψ_s and η_s values from the derived equations in Appendix B.

Define γ as the average (absolute) difference between values from the FE results and the stiffness equations expressed as a percentage of the FE value. I found that γ = 16.9 percent for the double-notched stringers and γ = 13.7 percent for the single-notched stringers when α = 5. By setting α = 3, the differences were reduced to γ = 5.7 and 5.4 percent for double- and single-notched stringers respectively. Furthermore, when α = 3, γ exceeds 10 percent mainly at the extreme notch depth D = 2.5 inches (ϕ = 0.667). At this depth the stiffness equations overestimate the FE predictions by 8 to 18 percent. Hirai and Sawada (1979a) also found the stiffness equations to overestimate measured midspan deflections of deeply notched beams. Notches in pallet stringers are seldom cut this deep. In figure 6 (center-point load), figure 7 (two-point load), and figure 8 (uniform load) this comparison is made graphically for the double-notched stringers with dimensions previously defined. For typical pallet stringer notch depths, the predictions of the stiffness equations (α = 3) and the experimentally verified FE model show close agreement. Furthermore, the stiffness equations are conservative for deeper notches.

Results for ψ_s indicate that the 'equivalent' notch geometry (α = 3) accurately estimates deflections at points other than midspan. Adequate prediction of deflection along the stringer length is required in a structural model of a pallet stringer. Figures 6-8 indicate that pallet stringers can be reliably and simply modeled with rectangular and tapered beam elements. The model can be further simplified by modeling the tapered elements with uniform elements of reduced stiffness (Kosko 1982).

I found the actual values of α that minimized γ were α = 2.2 (γ = 3.5 pct) and α = 2.0 (γ = 2.9 pct) for double- and single-notched stringers, respectively. Using these values, the fit is improved for the extreme notch depth of D = 2.5 inches (ϕ = 0.667) at the expense of worsening the fit at smaller notch depths which are common for pallet stringers. Thus, taking α = 3 is recommended. Pallet notches are substantially wider than the notches tested by Hirai and Sawada (1979a, 1979b). Also the range of ϕ considered in this paper is higher than the one considered by the two authors. Numerical results indicate that the best value for α depends on the range of ϕ considered. These reasons may explain why α = 3 is more suitable for notched pallet stringers than the value α = 5 found for other notched beams.

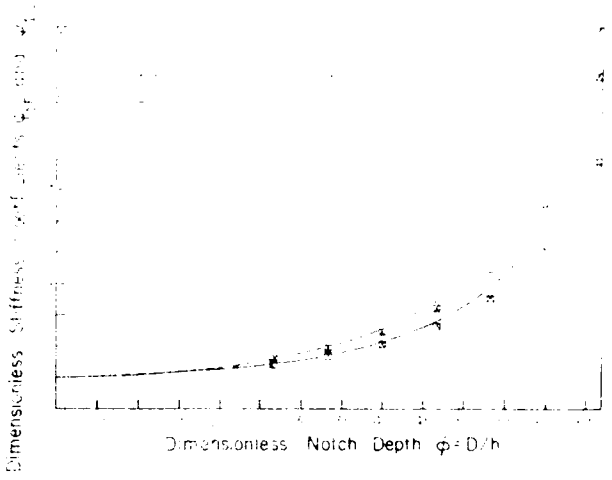

Figure 6 – Stiffness coefficients ψ_{1e} and ψ_{1o} versus ϕ for double-notched stringers under center-point load. Dimensions (see fig. 2): L = 48 inches, h = 3.75 inches, t = 1.5 inches, s = 44 inches, W = 9 inches, a = 9 inches, m = 4.5 inches, and q = 8.5 inches. (ML84 5501)

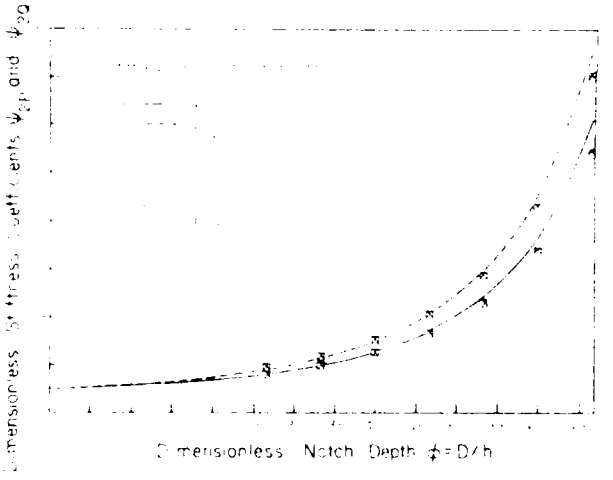

Figure 7 - Stiffness coefficients ψ_{2e} and ψ_{2o} versus ϕ for double-notched stringers under two-point load. Dimensions (see fig. 2): L = 48 inches, h = 3.75 inches, t = 1.5 inches, s = 44 inches, W = 9 inches, a = 9 inches, m = 4.5 inches, and q = 8.5 inches. (ML84 5502)

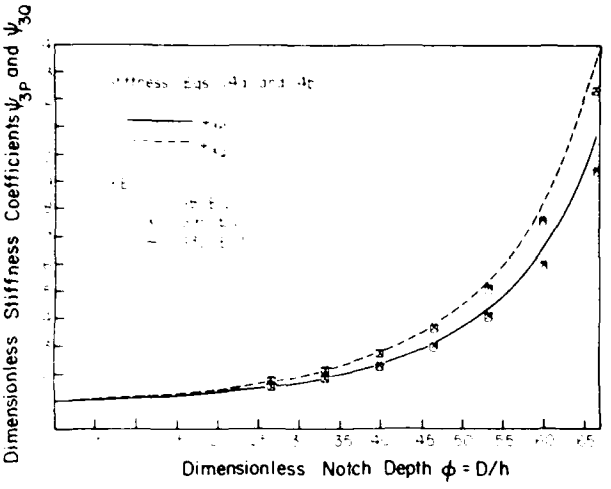

Figure 8.—Stiffness coefficients ψ_{3P} and ψ_{3O} versus for ϕ for double-notched stringers under uniform load. Dimensions (see fig. 2): ℓ = 48 inches, h = 3.75 inches, t = 1.5 inches, s = 44 inches, W = 9 inches, a = 9 inches, m = 4.5 inches, and q = 8.5 inches. (ML84 5503)

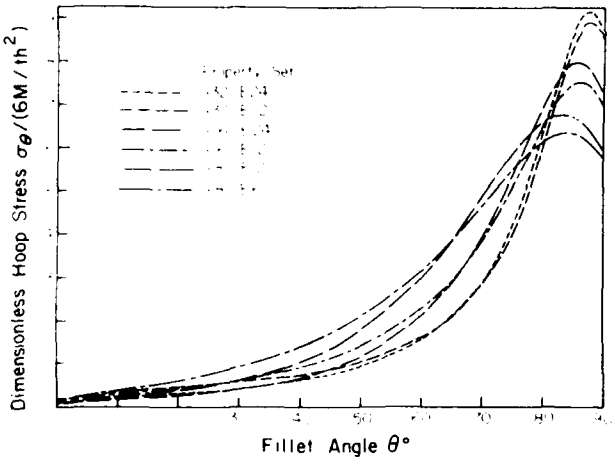

Figure 9.—Dimensionless hoop stress versus fillet angle for all six property sets. (ML84 5504)

As mentioned previously, computed FE deflections were sensitive to assumed $E_\ell/G_{\ell y}$ ratio. Computed FE ψ_n values, however, show little dependence on this ratio (figs. 6-8) due to the adjustment of MOE by equation (8). The stiffness equations thus appear adequate to model wood stringers with $E_\ell/G_{\ell y}$ ratios ranging from 8 to 32.

Fillet Stresses

The hybrid fillet element (Gerhardt 1984) directly computes the hoop stress along the fillet, σ_θ. The hoop stress can be readily resolved into stress components:

(1) along the grain (σ_x),
(2) perpendicular to the grain (σ_y), and
(3) shear (τ_{xy}) by

$$\begin{aligned} \sigma_x &= \sigma_\theta \sin^2\theta \\ \sigma_y &= \sigma_\theta \cos^2\theta \\ \tau_{xy} &= \sigma_\theta \sin\theta\cos\theta \end{aligned} \qquad (9)$$

The variable θ is the fillet angle shown in figure 5. The hoop stress distribution along the fillet is shown in figure 9 for a stringer (ℓ = 48 in., h = 3.75 in., t = 1.50 in.) with a center notch (fig. 1; W = 9.0 in., D = 1.5 in., ρ = 0.50 in.) loaded in quarter-point bending (s = 44 in., a = 11 in.). Results are presented for all six property ratios (table 4). For this loading condition, the fillet region is loaded in pure bending. Stress results are presented in dimensionless form $\sigma_\theta/(6M/th^2)$ where M is the resultant bending moment at the stringer cross section containing the fillet (θ = 90° in fig. 5).

The complexity of the stress distribution along the fillet is evident in figure 9. The magnitude of the maximum hoop stress, σ_{max}, depends on the assumed elastic property ratios. Computed σ_{max} is 44 percent greater for property set G32-E24 compared to set G8-E6. The locations of maximum σ_y and τ_{xy} along the fillet are distinct. In general, both differ from the location of σ_{max}. Furthermore, both location and magnitude of maximum σ_y and τ_{xy} depend on elastic property ratios, loading conditions, notch depth, and fillet radii.

In principle, equations for stringer strength could be derived by combining the stress distributions of figure 9, equation (9), and an interaction equation such as the one proposed by Norris (1962). The complexities cited in the previous paragraph, however, do not allow derivation of simple design equations by this approach. Fortunately, a suitable equation can be derived using only σ_{max} as will be shown later.

Maximum Hoop Stress as a Function of Notch Depth

Maximum hoop stress was computed for all the double- and single-notched FE stringer models described in the stiffness section. For these models, fillet radii was fixed at ρ = 0.50 inch. Two significant findings greatly simplified interpretation of the numerical results.

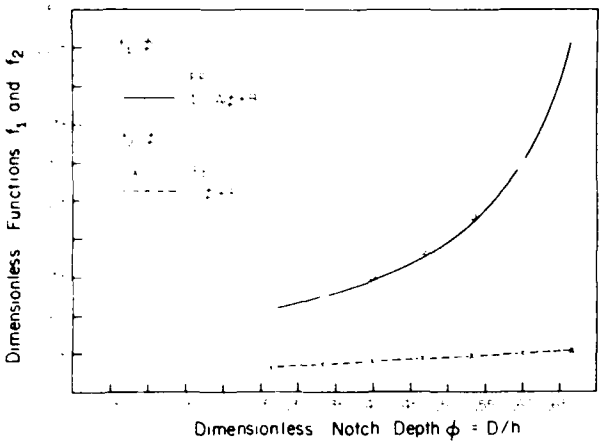

Figure 10.—Dimensionless functions f_1 and f_2 versus ϕ for property set G16-E12 (see eq. (10)). (ML84 5496)

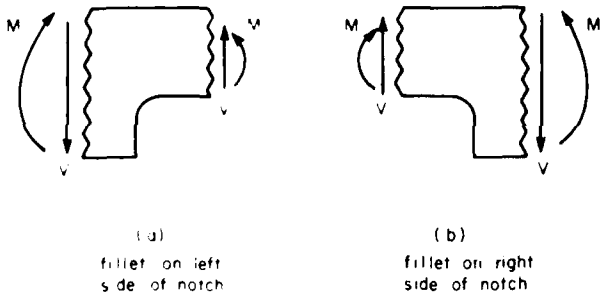

Figure 11.—Positive sign conventions for resultant bending moment (M) and shear force (V) at the stringer cross section containing the fillet. (ML84 5508)

(1) For all loading conditions σ_{max} could be approximated by an equation of the form

$$\sigma_{max} \quad (6M/th^2)\, f_1(\phi) + (6V/th)\, f_2(\phi) \qquad (10)$$

where

$f_1(\phi)$ and $f_2(\phi)$ are dimensionless functions of ϕ to be determined. M and V are defined as the resultant bending moment and shear force, respectively, at the stringer cross section containing the top of the fillet (at $\theta = 90°$ in fig. 5). M and V can be easily determined for any loading condition from shear and bending moment diagrams (Byars and Snyder 1975).

(2) Computed σ_{max} for single- and double-notched stringers differ by less than 0.6 percent if M, V, and ϕ are the same for both cases. For the geometries examined, the presence of a second notch negligibly increased fillet stress.

These two findings allow σ_{max} to be estimated for both single- and double-notched stringers under any loading condition once the functions $f_1(\phi)$ and $f_2(\phi)$ are determined.

The dependence of f_1 and f_2 on ϕ is indicated by the symbols in figure 10 for the property set G16-E12. I discovered that these tendencies can be approximated by the simple functions $1/(A\phi + B)$ for $f_1(\phi)$ and $(C\phi + F)$ for $f_2(\phi)$, where A, B, C, and F depend on assumed elastic property ratio. These coefficients were determined from least square fits to the FE results and are presented in table 5 for all six property ratios. The two functions are plotted as lines in figure 10. The derived equation for σ_{max} now takes the form

$$\sigma_{max} = (6M/th^2)[1/(A\phi + B)] + (6V/th)(C\phi + F) \qquad (11)$$

where $0.267 \leq \phi \leq 0.667$. The positive directions for M and V are both defined as to generate tensile fillet stresses. The positive sign conventions are illustrated in figure 11 for the two possible fillet orientations. Some care should be exercised in assigning the sign for V. Resultant shear forces in directions opposite to those shown in figure 11 will reduce σ_{max}. This effect will be seen later in the experimental results.

To examine the amount of error introduced by the closed form expression, predictions from equation (11) were compared to FE results. For each notch depth in each material set, σ_{max} was computed for six combinations of M and V (three different loading conditions for both single- and double-notched stringer FE models). Since 7 depths and 6 material sets were considered, 252 FE calculated σ_{max} were compared to equation (11). I found the difference (absolute) between equation (11) and FE calculations to be less than 5 percent (pct of FE σ_{max} value) for all notch depths except D = 2.5 inches ($\phi = 0.667$). For this extreme notch depth, equation (11) predictions exceed FE calculations by 12 to 15 percent. For all 252 comparisons, the mean absolute difference was 3.96 percent. Thus, equation (11) and table 5 reduce an enormous amount of FE calculations to a simple but accurate form.

Table 5.—Coefficients for equation (11)[1]

Material property set	A	B	C	F	A/B
G8-E6	-0.4148	0.3279	1.751	0.5218	-1.265
G8-E12	-.3868	.3064	2.330	.5150	-1.262
G16-E12	-.3494	.2766	2.815	.8485	-1.263
G16-E24	-.3281	.2604	3.449	.8535	-1.260
G32-E12	-.2973	.2351	4.525	1.322	-1.265
G32-E24	-.2872	.2277	4.981	1.297	-1.261

[1] For notches with fillet radii of ρ = 0.50 in.

Murphy (1979) plotted dimensionless stress intensity factors (both bending and shear) versus dimensionless crack length for split notched wood beams. It is worth noting that the curves proposed for $f_1(\rho)$ and $f_2(\rho)$ model the calculated stress intensity curves quite well for the range of ρ considered in this paper.

Maximum Hoop Stress as a Function of Fillet Radius

The dependency of σ_{max} on fillet radii ρ is examined in table 6 for a notch depth of D = 1.5 inches and property set G16-E12. Results are for loading with pure bending at the fillet (V = 0). This range of ρ represents the extremes of recommended fillet radius (NWPCA 1982). As expected, maximum hoop stress increases as the fillet radius increases. The magnitude of the change is fairly small. Results for ρ = 1.0 and 0.5 inch differ from the ρ = 0.75 inch results by only 15 percent and 8 percent, respectively.

Data presented in the following section indicate that varying ρ between 0.5 and 1.0 inch does not significantly affect strength of green oak stringers. Thus, for the objectives of this study, determination of the functional dependency of the coefficients in table 5 on ρ is not required. This dependency, however, can be readily determined from additional FE modeling if required.

Table 6.—Effect of fillet radii on maximum hoop stress[1]

ρ	$\sigma_{max}/(6M/th^2)$
(in)	
0.50	7.53
0.75	6.57
1.00	6.02

[1]Notch depth D = 1.5 in., property set G16-E12; resultant shear for a flat fillet V = 0.

Experimental Results and Discussion

Experimental results from tests of green oak pallet stringers are presented in this section. These results are compared with both FE calculations and the derived stiffness equations. An equation is derived to estimate stringer strength as a function of notch depth.

Material Properties

After mechanical testing, the measured moisture content (MC) of all stringers was above fiber saturation. The minimum MC was 42 percent, and mean MC for each of the 20 groups ranged from 58 to 68 percent.

MOE and MOR values were determined for the 3 unnotched groups of 30 stringers each. Mean, standard deviation (SD), coefficient of variation (COV), and 5th percentile values are presented in table 7. Ranges published in the Wood Handbook (USDA 1974) for small, clear specimens of green red oak are 1.18 to 1.79 million lb/in.^{2} for MOE, and 6,900 to 10,800 lb/in.^{2} for MOR. The values in table 7 fall into these ranges, but at the low end for MOE.

Single-Notched Stringers

The effects of notch depth, fillet radius, and loading condition on stringer stiffness and strength were examined by testing stringers with a single notch (fig. 1).

Stiffness

Deflections δ_P (at x = s/2) and δ_Q (at x = s/4) were measured for each stringer under a small load. MOE was computed for each board using δ_P and equation (5a) or (6a) with α = 3. In table 8 computed values are presented for stringer groups containing different notch depths (the first eight groups). If the stiffness equations reliably estimate the effect of notch depth, computed MOE will be independent of notch depth.

Consider first mean MOE values for stringer groups with notch depths of D = 1.0, 1.5, and 1.875 inches (see table 1). Analysis of variance indicated that the hypothesis of equal means could not be rejected since p = 0.38 for the three center-point loaded groups and p = 0.11 for the three quarter-point loaded groups.[2] The difference between the highest and lowest means is only 8 percent for the three center-point groups and 14 percent for the three quarter-point groups. This compares with differences of 11 and 19 percent, respectively, when α is taken as 5 in the stiffness equations. As indicated previously in comparison of FE results and the derived stiffness equations, use of α = 3 more reliably predicts stringer stiffness. Mean MOE values for the six groups, however, exceed unnotched MOE values by 11 to 28 percent. As mentioned before, the notched stringer groups contained a greater percentage of clear wood than the unnotched groups.

[2]The p value is defined as the probability that if the hypothesis (equal means) is true, the given (or larger) difference of means will be observed. Values of p less than 0.05, for instance, would imply that the difference in means is statistically significant at the 5 percent level.

Table 7.—Properties of unnotched stringers[1]

Group identification	Modulus of elasticity: Mean	Modulus of elasticity: 5th percentile	Modulus of elasticity: Standard deviation	Modulus of elasticity: Coefficient of variation	Modulus of rupture: Mean	Modulus of rupture: 5th percentile	Modulus of rupture: Standard deviation	Modulus of rupture: Coefficient of variation
	Million lb/in.²			Pct	Lb/in.²			Pct
M-C-1	1.20	0.760	0.233	19.5	7,360	4,350	1,470	19.9
C-C-1	1.24	.710	.248	20.0	8,730	5,500	1,980	22.7
C-C-2	1.17	.697	.253	21.6	8,240	5,830	1,350	16.4

[1] Dimensions and loading conditions given in table 3; 30 stringers per group.

Table 8.—Stiffness results for single-notched stringers[1] (fig. 1)

Group identification	[2]n	Modulus of elasticity[3]: Mean	Modulus of elasticity[3]: 5th percentile	Modulus of elasticity[3]: Standard deviation	Modulus of elasticity[3]: Coefficient of variation	REXP[4]: Mean	REXP[4]: Coefficient of variation	RFE[5]	RBT[6]: Mean	RBT/REXP: Mean	RBT/REXP: Coefficient of variation
		Million lb/in.²			Pct		Pct				Pct
C-D-1	30	1.37	0.944	0.266	19.4	1.55	4.1	1.61	1.58	1.02	4.2
C-D-2	30	1.38	.728	.331	24.0	1.61	2.8	1.66	1.63	1.02	2.9
C-D-3	30	1.48	.670	.379	25.6	1.66	2.6	1.69	1.67	1.01	2.6
C-D-4	28	1.60	.866	.374	23.4	1.73	1.8	1.74	1.71	.99	1.7
M-D-1	29	1.34	.863	.291	21.7	1.43	4.7	1.48	1.51	1.06	4.5
M-D-2	29	1.47	.778	.350	23.8	1.51	2.7	1.56	1.57	1.05	2.7
M-D-3	29	1.53	.781	.366	23.9	1.61	2.8	1.62	1.62	1.01	2.9
M-D-4	29	1.71	1.097	.339	19.8	1.69	3.8	1.70	1.68	1.01	4.3
M-R-1	30	1.52	1.125	.237	15.6	1.48	3.4	1.56	1.57	1.07	3.5
M-R-2	30	1.48	1.111	.237	16.0	1.48	2.5	1.57	1.57	1.06	2.5
M-R-3	30	1.40	.767	.302	21.6	1.51	2.9	1.57	1.57	1.04	2.8
M-R-0	30	1.38	.714	.295	21.4	1.50	3.2	—	1.58	1.05	3.2
M-S-1	30	1.47	.944	.279	19.0	1.46	3.9	—	—	—	—
M-S-2	30	1.35	.931	.207	15.3	1.45	2.7	—	-	—	—

[1] Dimensions and loading conditions given in table 1.

[2] Sample size.

[3] Modulus of elasticity computed from equation (5a) or (6a) and measured δ_P, where δ_P is the midspan deflection (at x = s/2)

[4] Experimentally measured δ_P/δ_Q, where δ_Q is the stringer deflection at x = s/4

[5] FE computed δ_P/δ_Q using mean geometry for each group and property set G16-E12

[6] Computed δ_P/δ_Q using derived stiffness equations with geometry of each stringer.

MOE means for groups C-D-4 and M-D-4 (notch depths of D = 2.5 inches or ξ = 0.667) are higher than those of the three associated groups with shallower notches. This can be attributed to the overestimation of η for extremely deep notches (ξ > 0.60). The overestimation was discussed earlier and is illustrated in figures 6-8 for double-notched stringers. Pallet stringers, however, are not normally notched this deeply.

MOE values vary substantially in a given group as evidenced by the SD and COV results in table 8. This variation makes comparison of measured deflections with FE results and stiffness equations rather difficult since a particular MOE is required to obtain either theoretical result. By considering the ratio δ_P/δ_Q, however, this difficulty can be overcome. The ratio is insensitive to MOE for stringers with constant MOE along the stringer length; the ratio is independent of MOE. Therefore, define three δ_P/δ_Q ratios

(1) REXP-experimentally measured,
(2) RBT-calculated from stiffness equations (5a), (5b), (6a), (6b) for each stringer, and
(3) RFE-calculated from FE model using mean stringer dimensions for each group.[7]

[7]The FE calculations were done with property set [illegible] sets with other E/G ratios [illegible] average.

REXP and RBT were compared for *each stringer* by computing the ratio RBT/REXP.

The following results were found by comparing the various δ_P/δ_Q ratios (see table 8). For each group:

(1) REXP had low COV values (1.8 to 4.7 pct) indicating the relative independence of δ_P/δ_Q on stringer MOE.

(2) RFE means differed from REXP means by only 0.6 to 3.5 *percent indicating* that the FE model accurately predicts stringer deflection. (This is also shown in App. A)

(3) RBT/REXP means range from 0.99 to 1.06 with COV of 1.7 to 4.5 *percent indicating* good agreement between the stiffness equations and the experimental measurements.

In summary, experimental results from full-size stringers indicate that the derived stiffness equations ($\alpha = 3$) reliably estimate beam deflections for both loading conditions when $\phi \leq 0.60$. Computed MOE values indicate that δ_P is reliably predicted. Consideration of the ratio δ_P/δ_Q indicates that deflection δ_Q is reliably predicted. For extremely deep notches ($\delta > 0.60$), the stiffness equations will calculate excessive deflections.

Computed MOE is affected little by fillet radius (table 8) as expected. Mean values ranged from 1.38 to 1.52 million lb/in.^{2}. Slits cut in groups M-S-1 and M-S-2 did not appreciably change MOE. Analysis of variance was done on MOE values for the last six groups in table 8 and group M-D-2 (same geometry as M-R-1 but cut on an industrial notcher). The hypothesis of equal means could not be rejected ($p = 0.18$).

Strength

The amount the ultimate load, P_u, exceeded the load at which the crack initiated at the fillet, P_i, was highly variable. For some stringers, knots caused cracks to propagate to an edge and P_u exceeded P_i only slightly. In more straight-grained stringers, the cracks propagated toward the stringer ends and stopped. These stringers did not break but experienced large deflection with decreasing load. For this type of failure mode, P_u was substantially greater than P_i. For a few cases, the difference was close to a factor of 2.

From measured P_i and P_u, resultant bending moments M_i (crack initiation load) and M_u (ultimate load) were calculated at the stringer cross section containing the fillet (at $\theta = 90°$ in fig. 5). Define normalized crack initiation and ultimate moments by $M_i^* = M_i/(th^2/6)$ and $M_u^* = M_u/(th^2/6)$, respectively. Dividing the moments by the section modulus of the unnotched portion of the stringers allows the moment capacity to be compared directly with the MOR results in table 7. Results for all 14 groups are presented in table 9. For a few stringers P_i could not be identified from the load deflection curve. M_i for these stringers was not included in the analysis, which explains the difference in sample size between crack initiation (n_i) and ultimate (n_u) moments.

Effect of fillet radius.—Results indicate that varying the fillet radius ρ (1/2, 3/4, and 1 in.) had negligible effect on both mean M_i^* (2,500, 2,640, and 2,590 lb/in.^{2}) and mean M_u^* (3,250, 3,110, and 3,010 lb/in.^{2}). The independence of fillet radius on crack initiation moment was somewhat unexpected since fillet stress does decrease as ρ increases (table 6). Apparently the magnitude of the stress decrease was insufficient to affect the crack initiation moment. Leicester (1974) also found the strength of slit-notched beams to be somewhat independent of notch root radii.

The group containing stringers with notches with sharp corners and no fillets (*M-R-0*) had mean values of $M_i^* = 1{,}960$ lb/in.^{2} and $M_u^* = 2{,}730$ lb/in.^{2}. These are approximately 24 and 12 percent less than the filleted groups. In comparing the unfilleted group to the filleted groups, the means could not be considered statistically equal for M_i^*($p < 0.0001$) but could be considered statistically equal for M_u^* at the 5 percent level ($p = 0.13$). However, comparing the 5th percentile values for M_u^*, the filleted groups exceed the unfilleted group by 17, 69, and 97 percent. The fillet apparently does have a beneficial effect on notched stringer performance, although all fillet radii between 0.5 and 1.0 inch yielded the same strength results in this study.

Table 9.—Critical normalized bending moments for single-notched stringers[1] (fig. 1)

Group identification	[2]n_i	M_i^*[3]				[4]n_u	M_u^*[5]				ϕ[6]
		Mean	5th percentile	Standard deviation	Coefficient of variation		Mean	5th percentile	Standard deviation	Coefficient of variation	Mean
		Lb/in.²			Pct		Lb/in.²			Pct	
C-D-1	29	3,430	1,790	681	19.9	30	4,040	2,690	747	18.5	0.266
C-D-2	26	2,410	1,560	440	18.3	30	2,710	1,620	562	20.7	.394
C-D-3	29	1,610	764	316	19.6	30	1,860	1,050	371	19.9	.509
C-D-4	25	800	454	152	19.0	28	903	592	169	18.7	.650
M-D-1	30	3,080	1,620	697	22.6	30	4,120	1,930	1,200	29.1	.269
M-D-2	30	2,340	1,260	490	20.9	30	2,990	1,600	898	30.0	.387
M-D-3	29	1,640	1,300	233	14.2	29	2,083	1,330	489	23.5	.504
M-D-4	30	885	678	138	15.6	30	1,010	719	266	26.3	.647
M-R-1	30	2,500	1,490	619	24.8	30	3,250	1,960	820	25.2	.384
M-R-2	29	2,640	1,900	372	14.1	30	3,110	2,290	501	16.1	.387
M-R-3	29	2,590	1,320	568	21.9	30	3,010	1,360	733	24.4	.393
M-R-0	30	1,960	1,130	398	20.3	30	2,730	1,160	725	26.6	.402
M-S-1	30	2,110	1,190	436	20.7	30	3,230	1,690	815	25.2	.391
M-S-2	30	1,930	1,180	433	22.4	30	3,150	1,470	904	28.7	.394

[1] Dimensions and loading conditions given in table 1.

[2] Sample size for crack initiation moments.

[3] $M_i^* = 6M_i/th^2$; where M is the resultant bending moment at the stringer cross section containing the top of the fillet ($\theta = 90°$ in fig. 5); M_i is M at the load the crack initiates.

[4] Sample size for ultimate moments.

[5] $M_u^* = 6M_u/th^2$; M_u is M at the ultimate load.

[6] $\phi = D/h$.

Effect of notch depth.—In figures 12 to 15, M_i^* and M_u^* are plotted versus dimensionless notch depth ϕ for all stringers in the first eight groups of table 9. The quarter-point and center-point loaded groups are presented in figures 12 and 13 and in figures 14 and 15, respectively. The variation of ϕ (D/h) in a given group is caused by variation in stringer height (h), not in notch depth (D). The two experimental lines in each figure are the regression line fitted using weighted least squares (Chatterjee and Price 1977), and the line for which 5 percent of the observations should lie below, if the errors are assumed to come from a normal distribution.

In contrast to the effect of fillet radius, figures 12 to 15 indicate that the moment capacity is strongly dependent on notch depth. In what follows, an equation that predicts mean M_i^* as a function of ϕ is derived from the FE results. The FE model cannot directly predict ultimate moment trends since a variety of failure modes can occur after crack initiation. The derived equation, however, will be modified to approximate 5th percentile estimates for both M_i^* and M_u^*. Design procedures for wood members are usually based on 5th percentile strength values.

First consider the four stringer groups loaded in quarter-point bending (figs. 12,13). These stringers have the notch region subjected to pure bending (V = 0). For this special case, equation (11) can be simplified to the form

$$\frac{6M}{th^2} = B\sigma_{max}\left(\frac{A}{B}\phi + 1\right) \qquad (12)$$

where $0.267 \le \phi \le 0.667$. Surprisingly, the ratio A/B is independent of assumed elastic property ratio as indicated in table 5. The ratio can be set equal to -1.26 with little error. Thus, equation (12) can be simplified to

$$\frac{6M}{th^2} = K(-1.26\phi + 1) \qquad (13)$$

where $0.267 \le \phi \le 0.667$ and $K = B\sigma_{max}$. Equation (13) can predict mean M_i^* as a function of ϕ by appropriately determining K. Define $\bar{K}_i$ as the value of K associated with crack initiation at the fillet, that is, at a particular value of σ_{max}. $\bar{K}_i$ can be obtained using mean values from *any* of the four quarter-point loaded groups. I chose group M-D-2 which has mean $M_i^* = 2{,}340$ lb/in.² and mean $\phi = 0.387$. Solving equation (13), one obtains $K = \bar{K}_i = 4{,}570$ lb/in.². Mean values from groups M-D-1, M-D-3, and M-D-4 compute $\bar{K}_i$ values that differ from this result by only 2.0, -1.7, and 4.8 percent, respectively. Thus, as predicted by the theory, $\bar{K}_i$ is independent of ϕ.

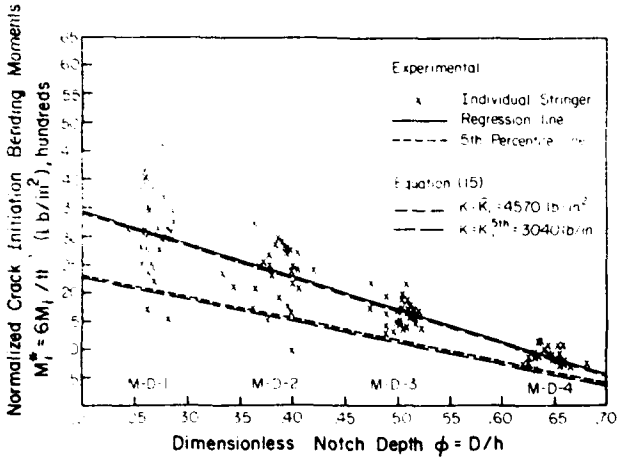

Figure 12.—Normalized crack initiation bending moments (M_i^*) versus ϕ for quarter-point loaded groups M-D-1, M-D-2, M-D-3, and M-D-4. (ML84 5497)

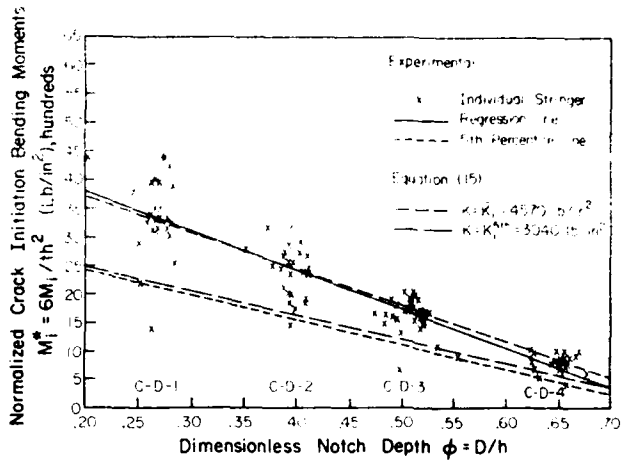

Figure 14.—Normalized crack initiation bending moments (M_i^*) versus ϕ for center-point loaded groups C-D-1, C-D-2, C-D-3, and C-D-4. (ML84 5499)

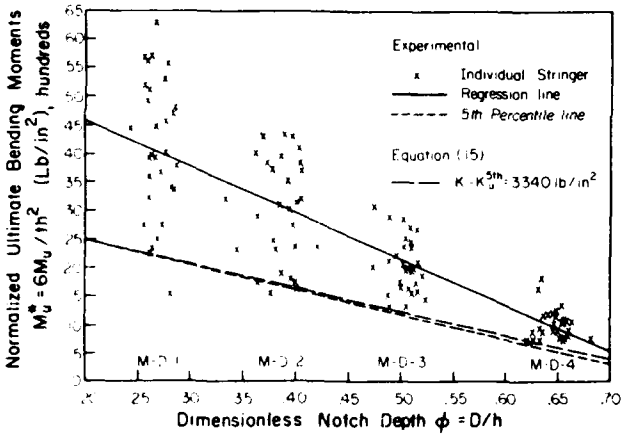

Figure 13.—Normalized ultimate bending moments (M_u^*) versus ϕ for quarter-point loaded groups M-D-1, M-D-2, M-D-3, and M-D-4. (ML84 5498)

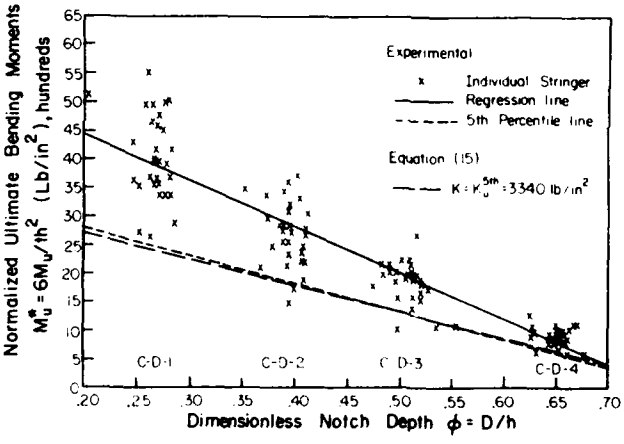

Figure 15.—Normalized ultimate bending moments (M_u^*) versus ϕ for center-point loaded groups C-D-1, C-D-2, C-D-3, and C-D-4. (ML84 5500)

Equation (13) is plotted in figure 12 with $K = \bar{K}_i = 4{,}570$ lb/in². The agreement of equation (13) with the regression line is excellent. The linear, elastic FE results correctly predict the slope of the line, i.e. the effect of notch depth on mean crack initiation moment. Note that a theory based on reduced section at the notch would predict that moment capacity is proportional to $(1 - \phi)^2$. The linear relation of equation (13) indicates that M_i^* is in fact related to stress concentration at the fillet and not a reduced section theory.

The discovery that the ratio A/B is independent of assumed elastic properties suggests that equation (13) can predict mean trends for other wood species. ($\bar{K}_i$ must be determined at one notch depth.) This hypothesis, however, must be experimentally confirmed before applying.

Equation (13) can be extended to handle any stringer loading condition as follows. Equation (11) can be now written as

$$K = \frac{6M}{th^2}\left[\frac{1}{-1.26\phi + 1}\right] + \frac{6V}{th}\left[CB\phi + FB\right] \qquad (14)$$

where 0.267 ≤ φ ≤ 0.667. Factors CB and FB vary somewhat with elastic property ratio (see table 5). The particular values chosen for CB and FB will not significantly change equation (14) since the moment term is much larger than the shear term. I used values from property set G32-E24. These will give the most conservative calculation of M when V is positive. (For double-notched stringers under most loading conditions, V will be positive.) Equation (14) can now be written

$$\frac{6M}{th^2} = \frac{1}{1.26\phi + 1} \cdot \frac{K}{\frac{Vh}{M}(1.13\phi + 0.30)} \qquad (15)$$

where 0.267 ≤ φ ≤ 0.667. Equation (15) clearly reduces to equation (13) when V = 0.

For any loading condition, the ratio V/M is known. For the four center-point loaded groups, V = P/2 (see sign convention, fig. 11) and M = P/2 x (22 - 4). Therefore V/M = 1/18 (in.$^{-1}$). This relationship is valid at both crack initiation and ultimate loads. To use equation (15) to predict mean M* simply set K = $\bar{K}$ = 4,570 lb/in.$^{3/2}$. Since $\bar{K}$ is related to a critical value of fillet stress, it is not dependent on stringer loading condition. Therefore, the value obtained from quarter-point loaded stringers is applicable. Equation (15) is plotted in figure 14 using K = $\bar{K}$ and a mean value for h of 3.78 inches. The agreement of the experimental regression line with equation (15) is quite good. Note that none of the data from center-point loading were used in constructing the theoretical line.

For this loading condition the resultant shear at the fillet reduces the maximum hoop stress (see eq. (11)). Comparing figure 14 with figure 12 indicates that both experiment and theory predict that the resultant shear increases the moment capacity.

By appropriately selecting K, equation (15) can also reliably calculate 5th percentile trends for both M* and M_5^*. Equation (15) is plotted on figures 12 and 13 (V/M = 0) and figures 14 and 15 (V/M = 1/18 in.$^{-1}$) using K = K^{5m} = 3,040 lb/in.$^{3/2}$ for crack initiation moment (figs. 12,14) and K = K_5^m = 3,340 lb/in.$^{3/2}$ for ultimate moment (figs. 13, 15). Agreement of these lines with regression lines is excellent.

In summary, a theoretical equation based on FE calculations was derived to predict mean crack initiation moment as a function of notch depth. The equation is based on the maximum fillet stress without regard to interaction of stresses such as tension perpendicular to grain and shear. Agreement of theoretical equation with experimental results was excellent for two loading conditions. By adjusting the value of K in equation (15), 5th percentile trends were accurately modeled for both M* and M_5^*. The load associated with a calculated critical bending moment can be readily obtained for any loading condition from the stringer bending moment diagram (Byars and Snyder 1975).

Effects of slits and cutting technique.—The slits cut at the fillet reduced mean M* by 10 and 18 percent (for two slit lengths) as compared to group M-D-2. Mean ultimate moments showed little difference as indicated in table 9. This result cannot be generalized to the problem of a crack at the fillet. Cracks initiated at the fillet from pallet nailing or stringer drying will be sharper than slits cut by a bandsaw. The effect of such cracks may be much more severe, therefore, additional research is required to resolve this issue.

The two cutting methods can be compared from results of groups M-R-1 and M-D-2. Stringers with notches cut at FPL (M-R-1) had higher strength values than stringers notched on the industrial equipment (M-D-2). Means were higher by 6.8 percent (M*) and 8.7 percent (M_5^*), while 5th percentiles were higher by 18.3 percent (M*) and 22.5 percent (M_5^*). The differences found, especially at the 5th percentile level, indicate that the effect of cutting technique on stringer strength may be another area that warrants further research.

Double-Notched Stringers

Equations that predict stringer stiffness and strength were previously derived. In this section the equations are compared with test results from three groups of double-notched stringers.

Stiffness

Stiffness results for double-notched stringers are presented in table 10. MOE was computed for each board using δ_p and equation (2a) or (3a) with α = 3. Mean MOE values for the three groups are 1.52, 1.45, and 1.28 million lb/in.^{2}. These means are similar to those found for single-notched stringers with notch depths of D = 1.0, 1.5, and 1.875 inches (see table 8). The deflection ratios in table 10 are defined as before except that δ_Q is measured at x = m ± 4.5 (see table 2 for m). The FE ratios (RFE) differ from the mean experimental ratios (REXP) by only 0.8, 1.3, and 4.0 percent. The agreement of the experimental ratios with the stiffness equation ratios (RBT) is also quite good since mean RBT/REXP values range from 0.97 to 1.05. Note that REXP increased from 1.49 to 1.72 as the span changed from 44 to 40 inches. This increase was accurately predicted by both the FE results and the stiffness equations.

Table 10.—Stiffness results for double-notched stringers[1] (fig. 2)

Group identification	[2]n	Modulus of elasticity[3]				REXP[4]		RFE[5]	RBT[6]	RBT/REXP	
		Mean	5th percentile	Standard deviation	Coefficient of variation	Mean	Coefficient of variation		Mean	Mean	Coefficient of variation
		Million lb/in.²			*Pct*		*Pct*				*Pct*
M-T-1	30	1.52	1.012	0.264	17.4	1.30	4.3	1.31	1.36	1.05	4.2
C-T-1	30	1.45	1.069	.191	17.9	1.49	4.0	1.47	1.47	.99	4.1
C-T-2	30	1.28	.736	.263	20.5	1.72	6.3	1.65	1.65	.97	6.2

[1] Dimensions and loading conditions given in table 2.

[2] Sample size.

[3] Modulus of elasticity computed from equation (2a) or (3a) and measured δ_P, where δ_P is the midspan deflection (at x = s/2).

[4] Experimentally measured δ_P/δ_Q, where δ_Q is the stringer deflection at x = m + 4.5 (see table 2 for m).

[5] FE computed δ_P/δ_Q using mean geometry for each group and property set G16-E12.

[6] Computed δ_P/δ_Q using derived stiffness equations with geometry of each stringer.

Table 11.—Normalized crack initiation moments for double-notched stringers[1] (fig. 2)

Group identification	[2]n_i	M_i^*[3]				ϕ	h	Computed[4] M_i^*	
		Mean	5th percentile	Standard deviation	Coefficient of variation	Mean	Mean	Mean	5th percentile
		Lb/in.²			*Pct*		*In.*	*Lb/in.²*	*Lb/in.²*
M-T-1	28	2,460	1,410	472	19.2	0.383	3.75	2,360	1,570
C-T-1	29	2,100	1,540	298	14.2	.379	3.74	2,150	1,430
C-T-2	30	1,870	1,140	429	22.9	.381	3.74	2,100	1,400

[1] Dimensions and loading conditions given in table 2.

[2] Sample size.

[3] $M_i^* = 6M_i/th^2$, where M is the resultant bending moment at the stringer cross sections containing the fillets closest to midspan, M_i is M at the load the crack initiates.

[4] Computed from equation (15) with $K = \bar{K}_i = 4,570$ lb/in.$^{3/2}$ for the mean values and with $K = K_i^{5th} = 3,040$ lb/in.$^{3/2}$ for the 5th percentile values.

Table 12.—Normalized ultimate moments for double-notched stringers[1] (fig. 2)

Group identification	[2]n_u	M_u^*[3]				Computed[4] M_u^*
		Mean	5th percentile	Standard deviation	Coefficient of variation	5th percentile
		Lb/in.²			*Pct*	*Lb/in.²*
M-T-1	30	3,070	1,890	777	25.3	1,730
C-T-1	30	2,230	1,320	447	20.0	1,570
C-T-2	30	2,000	1,210	451	22.6	1,540

[1] Dimensions and loading conditions given in table 2.

[2] Sample size.

[3] $M_u^* = 6M_u/th^2$, where M is the resultant bending moment at the stringer cross sections containing the fillets closest to midspan, M_u is M at the ultimate load.

[4] Computed from equation (15) with $K = K_u^{5th} = 3,340$ lb/in.$^{3/2}$

Strength

Experimental results are presented in table 11 for crack initiation moments and in table 12 for ultimate moments. The bending moments are computed at the fillets nearest midspan. Cracks always initiated at one of these two fillets because they were subjected to much higher bending moments than the fillets closest to the supports. Equation (15) was used to calculate mean M_i^* (K = 4,570 lb/in.^{2}) and 5th percentile values for M_i^* (K = 3,040 lb/in.^{2}) and M_u^* (K = 3,340 lb/in.^{2}). The appropriate values for V/M are 0 (M-T-1), 13 in.$^{-1}$ (C-T-1), and 11 in.$^{-1}$ (C-T-2). The predicted mean M_i^* values differ from the experimental values by only 4.0, 2.4, and 12.3 percent. The theory thus reliably predicts mean crack initiation moments for double-notched stringers. The center-point loading resulted in positive resultant shear forces at the fillets nearest midspan. These forces increased fillet stresses and reduced moment capacity as compared to the two-point loaded group. This reduction was predicted by both theory and experiment.

The differences between experimental and predicted 5th percentile values were 11, 7, and 23 percent for M_i^* and 8, 19, and 27 percent for M_u^*. Differences of this magnitude are quite acceptable since the sample sizes (about 30 stringers/group) are small. Fifth percentile regression lines for single-notched groups were based on about 120 data points. Although the agreement between equation (15) and these lines was excellent, the magnitude of differences between experimental and predicted 5th percentile values for individual groups were similar to those found for double-notched stringers.

Effect of Span

Results from group C-T-2 examine the effect of reducing span on stringer stiffness and strength. The span of notched stringers is somewhat adjustable since pallets are often supported across the stringers in warehouse racks. Stiffness changes are examined in table 13 as the span is reduced from 44 inches to 42 and then to 40 inches. Calculations were made using stiffness equations (2a) and (4a) with α = 3. The reductions in center deflection are based on percent of the value when s = 44 inches. Based on beam theory, reductions for unnotched beams would be 13 percent (s = 42 in.) and 24.9 percent (s = 40 in.).

Table 13.—Effect of span on center deflection of double-notched stringers[1] (fig. 2)

D	[2]ϕ	Reduction in center deflection[3]			
		Center-point load		Uniform load	
		s = 42 inch	s = 40 inch	s = 42 inch	s = 40 inch
In.		*Pct*		*Pct*	
1.00	0.267	14.7	27.9	19.5	32.0
1.25	.333	15.2	28.8	21.4	34.0
1.50	.400	15.7	29.7	23.1	35.9
1.75	.467	16.1	30.5	24.7	37.6
2.00	.533	16.6	31.3	26.0	39.1

[1] Dimensions: h = 3.75 in., q = 8.5 in., W = 9.0 in.

[2] ϕ = D/h.

[3] As compared to span of s = 44 in.

For center-point loading, reducing span actually decreases moment capacity at the fillet as indicated by experimental and theoretical results in tables 11 and 12. This reduction is caused by an increased shear contribution (higher V/M ratio) to fillet stresses. Although the moment capacity at the fillet decreases, the load carrying capacity of the stringer does increase as span is reduced. The increased load capacity is caused by altered relationships between load and fillet bending moment. Load capacity changes can be easily calculated from equation (15) and stringer bending moment diagram. I found that decreasing the span from 44 inches to 42 and then to 40 inches increased load capacity by 7.5 and 16 percent for center-point loading and by 6.8 and 15 percent for uniform loading.

Conclusions

The conclusions from this study of notched, green oak pallet stringers are presented separately for stringer stiffness and strength. For stringer stiffness:

(1) Results from a FE structural model show excellent agreement with experimental results from both full-size and small-scale (see fig. A1) notched pallet stringers.
(2) Results from derived stiffness equations (2-7) agree well with FE results for notch depths associated with pallet stringers. The stiffness equations are based on a structural model that utilizes rectangular and tapered beam elements with an 'equivalent' notch geometry.
(3) Results from tests of full-size notched stringers indicate the derived stiffness equations (2-7) accurately predict the effect of notch depth on stringer stiffness.
(4) Experimental results indicate that stringer stiffness is independent of fillet radii.

For stringer strength:
(1) Experimental results indicate that stringer strength is unaffected by varying the fillet radii from 1/2 to 1 inch. A group of stringers with sharp, rectangular notches (no fillet) did have lower strength than the filleted groups.
(2) Experimental results indicate that stringer strength is quite sensitive to notch depth. Equation (15) predicts moment capacity as a function of notch depth for any loading condition. It was derived from FE stress results. Equation (15) predicts both mean and 5th percentile strengths that show excellent agreement with experimental results.

In summary, pallet stringers can be structurally modeled by utilizing beam elements of the 'equivalent' geometry (fig. 3). These elements will model stringer stiffness quite accurately. Using this 'equivalent' geometry, a node [illegible] rectangular and tapered beam elements will exist at every fillet. Thus, when used as part of a pallet structure, the resultant bending moment (M) and shear force (V) will be computed at every stringer cross section containing a fillet. From M and V and equation (15), mean or 5th percentile failure loads can be predicted for any notch geometry and pallet loading condition.

Literature Cited

Bastendorff, K. M.; Polensek, A. Working stresses for red alder and bigleaf maple pallet materials. Project F-818-130. Corvallis, OR: Oregon State University, School of Forestry, Department of Forest Products; 1981.

Bastendorff, K. M.; Polensek, A. Strength and stiffness of red alder and bigleaf maple pallet materials. Forest Products Journal 34(7/8): 51-56; 1984.

Bodig, J.; Goodman, J. R. Prediction of elastic parameters for wood. Wood Science. 5(4): 249-264; 1973.

Byars, E. F.; Snyder, R. D. Engineering mechanics of deformable bodies. 3d. ed. New York: Intext Educational Publishers; 1975. 504 p.

Chatterjee, S.; Price, B. Regression analysis by example. New York: John Wiley and Sons, Inc.; 1977: 101-107.

Forest Products Laboratory, Forest Service. Wood handbook: Wood as an engineering material. Agric. Handb. 72. Washington, DC: U.S. Department of Agriculture; rev. 1974. 432 p.

Gerhardt, T. D. Plane stress analysis of wood members using isoparametric finite elements—a computer program. Gen. Tech. Rep. FPL -35. Madison, WI: U.S. Department of Agriculture, Forest Service, Forest Products Laboratory; 1983. 16 p.

Gerhardt, T. D. A hybrid/finite element approach for stress analysis of notched anisotropic materials. Accepted for publication in ASME Journal of Applied Mechanics; 1984.

Gerhardt, T. D.; Liu, J. Y. Orthotropic beams under normal and shear loading. Journal of Engineering Mechanics. 109(2): 394-410; 1983.

Hearn, A. C. Reduce 2 user's manual. UCP-19. Salt Lake City, UT: University of Utah; 1973.

Hirai, T.; Sawada, M. Stiffness and load carrying capacity of square-notched beams 1. On the estimation of the effective stiffness. Research Bulletins of the College Experiment Forests, College of Agriculture, Hokkaido University XXXVI(2): 387-420. Sapporo, Japan; 1979a.

Hirai, T.; Sawada, M. Stiffness and load carrying capacity of square-notched beams 2. On the applicability of the equivalent notch method. Research Bulletins of the College Experiment Forests, College of Agriculture, Hokkaido University XXXVI(3): 663-680. Sapporo, Japan; 1979b.

Hirai, T.; Sawada, M. Stiffness and load carrying capacity of square-notched wood beams 3. On the maximum failure moments. Research Bulletins of the College Experiment Forests, College of Agriculture, Hokkaido University XXXVII(3): 759-788. Sapporo, Japan; 1980.

Kosko, E. Uniform element modeling of tapered frame members. Journal of the Structural Division, Proceedings American Society of Civil Engineers. 108(ST1): 245-264; 1982.

Leicester, R. H. Fracture strength of wood. First Australian conference of engineering materials, The University of New South Wales; 1974.

Leicester, R. H.; Poynter, W. G. On the design strength of notched beams. In: Proceedings, IUFRO conference. Wood Engineering Group; 1980 April; Oxford, UK.

McKeever, D. B.; Hatfield, C. A. Trends in the production and consumption of major forest products in the United States. Resour. Bull. FPL 14. Madison, WI: U.S. Department of Agriculture, Forest Service, Forest Products Laboratory; 1984. 59 p.

McLain, T. E. Personal communication. Associate Professor, Wood Engineering. Blacksburg, VA: Virginia Polytechnic Institute and State University; May 4, 1982.

Murphy, J. F. Using fracture mechanics to predict failure in notched wood beams. In: Proceedings, First international conference on wood fracture; 1978 August; Banff, Alberta; 1979: 159-173.

National Wooden Pallet and Container Association. Hardwood pallet standards. Washington, DC: NWPCA; 1982.

Norris, C. B. Strength of orthotropic materials subjected to combined stresses. Res. Rep. No. 1816. Madison, WI: U.S. Department of Agriculture, Forest Service, Forest Products Laboratory; 1962. 24 p.

Orosz, I. Simplified method for calculating shear deflections of beams. Res. Note FPL-0210. Madison, WI: U.S. Department of Agriculture, Forest Service, Forest Products Laboratory, 1970. 12 p.

Palka, L. C.; Holmes, B. Tangential failure of small wood cantilevered beams with square notches. Wood Science. 5(3): 172-180, 1973.

Peterson, R. E. Stress concentration factors. New York: John Wiley and Sons; 1974. 314 p.

Richards, D. B. Strength of wood beams with shallow curved notches. Wood Science. 7(1): 77-84; 1974.

Seely, F. B.; Smith J. O. Advanced mechanics of materials. 2d ed. New York: John Wiley and Sons; 1955. 680 p.

Stern, E. G. Nail-reinforced pallet stringers, a pilot study. Bull. No. 111. Blacksburg, VA: Virginia Polytechnic Institute and State University; 1972.

Stieda, C.K.A. Stress concentrations around holes and notches and their effect on the strength of wood beams. Journal of Materials. 1(3): 560-582; 1966.

Timoshenko, S. P.; Goodier, J. N. Theory of elasticity. 3d ed. New York: McGraw-Hill; 1970. 567 p.

Wallin, W. B.; Stern, E. G.; Johnson, J. A. Determination of flexural behavior of stringer-type pallets and skids. Bull. No. 146. Blacksburg, VA: Virginia Polytechnic Institute and State University; 1976.

Zienkiewicz, O. C. The finite element method. 3d ed. London: McGraw Hill; 1977. 787 p.

Appendix A—Comparison of Finite Element Results With Experimental Measurements

A finite element (FE) mesh similar to figure 5 was constructed to model a small (ℓ = 11.375 in., h = 1.5 in., t = 0.25 in.) single-notched (D = 0.5 in., W = 2.5 in., ρ = 0.1875 in.) Sitka spruce stringer loaded in center-point bending.[4] Computed and measured center displacement[4] is shown in figure A1. The agreement is excellent, validating the FE model for stiffness computation. Strains were also measured in the spruce stringer when loaded in tension.[4] Experimental and computed normal strains compared favorably except at the fillet tip. At this location, the linear elastic model could not predict the apparent nonlinear response.

I compared FE results with published photoelasticity results to insure that the fillet element computed accurate, linear elastic stresses. Experimental results for a tensile-loaded stepped bar with shoulder fillets are presented in figure 65 (Peterson 1974). The problem can be modeled by the mesh of figure 5 with vertical symmetry imposed along the top surface. Since the formulation for the hybrid element is anisotropic, near isotropic properties were used in the analysis, i.e., $E_y/E_x = 1.001$, $G_{xy}/E_x = 0.4$, ν_{xy} = 0.25. The fillet radius (ρ) and notch depths (D) chosen are shown in table A1. These approximate the ranges needed in modeling the notched stringer. The mesh used was identical to figure 5 with h = 4.0 inches, except that six 12-node cubic elements were added to the left side to insure uniform tension at the end.

Computed and experimental stress concentration factors, K_T, are compared in table A1. K_T is defined as maximum fillet stress divided by nominal tensile stress in the narrow section of bar. Computed and measured K_T differ by less than 4.5 percent for all nine cases. Varying Ω by 0.5 to 1.5 times changed computed K_T by a few percent. Values shown in table A1 agreed best with experimental results. These scalings were used in the notched stringer models.

The hybrid element contains 13 nodes. Thus, the minimum number of terms required in the assumed Taylor series expansion is 12 (Gerhardt 1984). This minimum number was used in the results presented in table A1. Results from using 13-17 terms changed K_T by only tenths of a percent. Finally, 20 gauss points were used to integrate each side of the hybrid element (Gerhardt 1984). This level of quadrature resulted in stress convergence to five decimal points. In conclusion, the photoelasticity results indicate that the scaling used in figures 4 and 5 will compute reliable elastic stresses over the desired ranges of D and ρ.

[4] Wyatt, J. B., Gerhardt, T. D., Peterson, R. A., Rowlands, R. E. Stiffness and strains in wood beams having rectangular filleted notches. In preparation. Forest Service, Forest Products Laboratory, Madison, WI: USDA.

Table A1—Comparison of finite element (FE) and photoelasticity results[1]

D	ρ	Ω	$^2K_{T_{FE}}$	$^3K_{T_{EXP}}$	Difference
---------- *In.* ----------					*Pct*
2.00	0.50	0.50	2.330	2.26	3.1
2.00	.75	.50	2.026	1.99	1.8
2.00	1.00	.75	1.835	1.84	.3
1.33	.50	.50	2.358	2.29	3.0
1.33	.75	.50	2.061	2.03	1.5
1.33	1.00	.75	1.915	1.87	2.4
.923	.50	.50	2.278	2.18	4.5
.923	.75	.50	2.004	1.96	2.2
.923	1.00	.75	1.843	1.82	1.3

[1] Results for a tensile-loaded stepped bar with shoulder fillets, i.e. fig. 5 (h = 4.0 in.) with symmetry imposed along y = h and loaded in uniform tension in the x-direction.

[2] $K_T = \sigma_{max}/T$, where σ_{max} = maximum stress along fillet and T = tensile stress applied to narrow section of bar.

[3] Photoelasticity values estimated from fig. 65 in Peterson (1974).

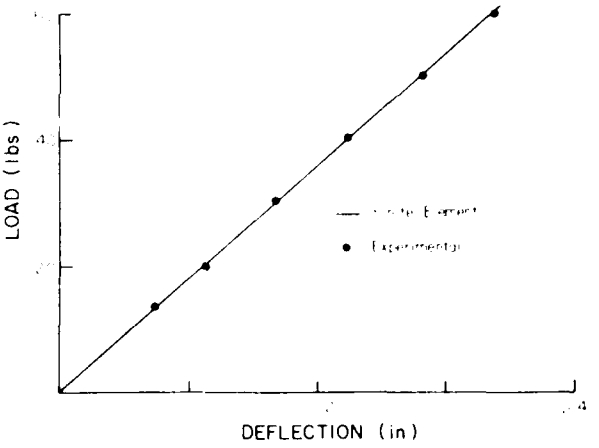

Figure A1—Comparison of FE and experimental midspan deflection for a small, single-notched stringer. (ML84 5506)

Appendix B—Definition of Dimensionless Factors for Equations (2-7)

Dimensionless factors ψ_{ij} for double-notched stringers (fig. 2) are defined as follows:

$$\psi_{11} = \frac{8(n_0^3 - m_0^3)}{(1-\phi)^3} + \frac{12\alpha h_0(\beta_0^2 + \gamma_0^2)}{(1-\phi)^2} + \frac{48\alpha^2h_0^2(\beta_0 + \gamma_0)}{(1-\phi)} + 12\alpha h_0 C_1 + 48\alpha^2h_0^2C_2 + 12\alpha^3h_0^3C_3 + C_4$$

$$\psi_{12} = \frac{1}{a_0(3+4a_0^2)}\left[\frac{12n_0^2a_0 - 8m_0^3 + 4a_0^3}{(1-\phi)^3} + \frac{12\alpha h_0(\beta_0^2 + \gamma_0^2 a_0)}{(1-\phi)^2} + \frac{24\alpha^2h_0^2(a_0 + 2\beta_0)}{(1-\phi)} + 12\alpha C_5 + 24\alpha^2h_0^2C_6 + 12\alpha^3h_0^3C_7 + C_8\right]$$

$$\psi_{21} = \psi_{12}$$

$$\psi_{22} = \frac{1}{a_0^2(3+4a_0^2)}\left[\frac{6n_0a_0^2 - 2m_0^3 + 4a_0^3}{(1-\phi)^3} + \frac{3\alpha h_0(\beta_0^2 + a_0^2)}{(1-\phi)^2} + \frac{12\alpha^2h_0^2\beta_0}{(1-\phi)} + 3\alpha h_0 C_9 + 12\alpha^2h_0^2C_{10} + 3\alpha^3h_0^3C_{11} + C_{12}\right]$$

$$\psi_{23} = 0.2\left[\frac{16n_0^3(4 - 3n_0) + m_0^3(4 + 3m_0)}{(1-\phi)^3} + \frac{96\alpha h_0\beta_0^2(1-\phi) + 96\alpha h_0\gamma_0^2(1+\phi)}{(1-\phi)^2} + \frac{192\alpha^2h_0^2\beta_0(2 + 3\beta_0 - \gamma_0^2)}{(1-\phi)} + 96\alpha h_0 C_{13} + 192\alpha^2h_0^2C_{14} + 96\alpha^3h_0^3C_{15} + C_{16}\right]$$

$$\psi_{33} = \frac{1}{a_0(1+2a_0^2+a_0^3)}\left[\frac{a_0^3(2 + a_0) + m_0^3(4 + 3m_0) + 2n_0^3a_0(3 - 2n_0)}{(1-\phi)^3} + \frac{6\alpha h_0\beta_0(1-\phi) + 3\alpha h_0(1+\phi)}{(1-\phi)^2} + \frac{12\alpha^2h_0^2\beta_0(2 + 3\beta_0) + a_0(1 + 2\gamma_0^2)}{(1-\phi)} + 6\alpha h_0 C_{17} + 12\alpha^2h_0^2C_{18} + 6\alpha^3h_0^3C_{19} + C_{20}\right]$$

The dimensionless constants are defined by (see fig. 2): $\phi = D/h_0$; $n_0 = (m_0 + W)/s_0$; $h_0 = h/s_0$; $a_0 = a/s_0$; $m_0 = m/s_0$; $m_0 + W/s_0$ (1 - ϕ); and $\gamma_0 = n_0 + \alpha h_0(1 - \phi)$. The constants C_i (i = 1,20) are defined in table B1.

Dimensionless factors κ_{ij} for single-notched stringers (fig. 1) are defined as follows:

$$\kappa_{11} = \frac{1}{(1-\phi)^3} + \frac{8m_0^3}{(1-\phi)^3} + \frac{12\alpha h_0\beta_0^2}{(1-\phi)^2} + \frac{48\alpha^2h_0^2\beta_0}{(1-\phi)} + 12\alpha h_0 K_1 + 48\alpha^2h_0^2K_2 + 12\alpha^3h_0^3K_3 + K_4$$

$$\kappa_{12} = \frac{1}{(3+4a_0^2)}\left[\frac{3}{(1-\phi)^3} + \frac{12m_0^2}{(1-\phi)^3} + \frac{12\alpha h_0\beta_0}{(1-\phi)^2} + \frac{24\alpha^2h_0^2}{(1-\phi)} + 12\alpha h_0 K_5 + 24\alpha^2h_0^2K_6 + K_7\right]$$

$$\kappa_{21} = \kappa_{12}$$

$$\kappa_{22} = \frac{1}{(3+4a_0^2)}\left[\frac{3}{(1-\phi)^3} + \frac{6m_0}{(1-\phi)^3} + \frac{3\alpha h_0}{(1-\phi)^2} + 3\alpha h_0 K_8 + K_9\right]$$

$$\kappa_{23} = 0.2\left[\frac{5 + 16m_0^3(4 - 3m_0)}{(1-\phi)^3} + \frac{96\alpha h_0\beta_0^2(1-\phi)}{(1-\phi)^2} + \frac{192\alpha^2h_0^2\beta_0(2 + 3\beta_0)}{(1-\phi)} + 96\alpha h_0 K_{10} + 192\alpha^2h_0^2K_{11} + 192\alpha^3h_0^3K_{12} + K_{13}\right]$$

$$\kappa_{33} = \frac{1}{(1+2a_0^2+a_0^3)}\left[\frac{1 + 2m_0^3(3 + 2m_0)}{(1-\phi)^3} + \frac{6\alpha h_0\beta_0(1-\phi)}{(1-\phi)^2} + \frac{12\alpha^2h_0^2(1 + 2\beta_0)}{(1-\phi)} + 6\alpha h_0 K_{14} + 12\alpha^2h_0^2K_{15} + 12\alpha^3h_0^3K_{16} + K_{17}\right]$$

The dimensionless constants are defined by (see fig. 1): $\phi = D/h_0$; $h_0 = h/s_0$; $a_0 = a/s_0$; $m_0 = m/s_0$; and $\gamma_0 = m_0 + \alpha h_0(1 - \phi)$. The constants K_i (i = 1,17) are defined in table B2.

Table B1—Relationships for constants C_i (i = 1,20)

	Appropriate notch depth interval		
	[1] I_1	[2] I_2	[3] I_3
[4] C_1	$\beta_o^2 + \gamma_o^2$	γ_o^2	$\gamma_o^2\theta_1^2$
C_2	$\beta_o + \gamma_o$	γ_o	$\gamma_o\theta_1$
[5] C_3	$-4\ell n(1 - \phi)$	$3 - 2\ell n(1 - \phi) - 2\ell n(\theta_2)$	$3 - 2\ell n(\theta_2) - 2\ell n(\theta_3)$
[6] C_4	$1 + 8(x_t^3 - x_r^3)$	$1 - 8x_r^3$	0
C_5	$\gamma_o a_o - \beta_o^2$	$\gamma_o a_o$	$\gamma_o a_o\theta_1^2$
C_6	$-2\beta_o + a_o$	a_o	$a_o\theta_1$
C_7	$-2\ell n(1 - \phi)$	$3 - 2\ell n(\theta_2)$	$3 - 2\ell n(\theta_2)$
C_8	$3a_o + 8x_t^3 - 12x_r^2a_o$	$3a_o - 12x_r^2a_o$	0
C_9	$\beta_o^2(-1 + \beta_o) - \gamma_o^2(1 + \gamma_o)$	$-\gamma_o^2(1 + \gamma_o)$	$-\gamma_o^2(1 + \gamma_o)\theta_1^2$
C_{10}	$\beta_o(2 - 3\beta_o) + \gamma_o(2 + 3\gamma_o)$	$\gamma_o(2 + 3\gamma_o)$	$\gamma_o(2 + 3\gamma_o)\theta_1$
C_{11}	$-4 + 6(\beta_o - \gamma_o)\ell n(1 - \phi)$	$3 + 2m_o - 5\beta_o - 2\alpha\phi h_o - 2(1 + 3\gamma_o)\ell n(1 - \phi) - 2(1 - 3\beta_o)\ell n(\theta_2)$	$2 + 2m_o + 2n_o - 5\beta_o - 2(1 + 3\gamma_o)\ell n(\theta_3) - 2(1 - 3\beta_o)\ell n(\theta_2)$
C_{12}	$5 + 16x_r^3(-4 + 3x_r) + 16x_t^3(4 - 3x_t)$	$5 + 16x_r^3(-4 + 3x_r)$	0
C_{13}	$\beta_o^2 + a_o^2$	a_o^2	$a_o^2\theta_1^2$
C_{14}	β_o	0	0
C_{15}	$-2\ell n(1 - \phi)$	$3 - 2\ell n(\theta_2)$	$3 - 2\ell n(\theta_2)$
C_{16}	$3a_o^2 + 2x_t^3 - 6x_ra_o^2$	$3a_o^2 - 6x_ra_o^2$	0
C_{17}	$\beta_o^2(-1 + \beta_o) + \gamma_oa_o(1 + \gamma_o)$	$\gamma_oa_o(1 + \gamma_o)$	$\gamma_oa_o(1 + \gamma_o)\theta_1^2$
C_{18}	$\beta_o(2 - 3\beta_o) - a_o(1 + 2\gamma_o)$	$-a_o(1 + 2\gamma_o)$	$-a_o(1 + 2\gamma_o)\theta_1$
C_{19}	$2(-1 + a_o + 3\beta_o)\ell n(1 - \phi) + 2m_o - 2x_t$	$2a_o\ell n(1 - \phi) + 2(-1 + 3\beta_o)\ell n(\theta_2) + 3 + 2m_o - 5\beta_o$	$2a_o\ell n(\theta_3) + 2(-1 + 3\beta_o)\ell n(\theta_2) + 3 + 2m_o - 5\beta_o$
C_{20}	$a_o + x_t^3(4 - 3x_t) + 2x_r^2a_o(-3 + 2x_r)$	$a_o + 2x_r^2a_o(-3 + 2x_r)$	0

[1] I_1: $D \leq m/\alpha$ and $D \leq q/\alpha$ (see fig. 2)

[2] I_2: $D > m/\alpha$ and $D \leq q/\alpha$

[3] I_3: $D > m/\alpha$ and $D > q/\alpha$

[4] $\theta_1 = 2\alpha h_o/(1 + 2\gamma_o)$

[5] $\theta_2 = \alpha h_o(1 - \phi)/\beta_o$; $\theta_3 = (1 - \phi)\theta_1$

[6] $x_t = \beta_o - \alpha h_o$; $x_r = -\gamma_o + \alpha h_o$

Table B2—Relationships for constants K_i ($i = 1,17$)

	Appropriate notch depth interval	
	[1] I_1	[2] I_2
K_1	β_o^2	Same
K_2	β_o	Same
K_3	$2\ell n(1 - \phi)$	Same
[3] K_4	$8x_\ell^3$	Same
[4] K_5	β_o	$\beta_o[(a_o - \beta_o)\theta_4^2 + \beta_o]/a_o$
K_6	1	$[(a_o - 2\beta_o)\theta_4 + 2\beta_o]/a_o$
K_7	$12x_\ell^2 - 4a_o^2$	$[24\alpha^3 h_o^3 \ell n(\theta_4) + 8x_\ell^3]/a_o$
K_8	$\beta_o^2(1 + \beta_o)$	Same
K_9	$\beta_o(2 - 3\beta_o)$	Same
K_{10}	$m_o - x_\ell + (-1 + 3\beta_o)\ell n(1 - \phi)$	Same
K_{11}	$16x_\ell^3(4 - 3x_\ell)$	Same
K_{12}	1	$[(a_o^2 - \beta_o^2)\theta_4^2 + \beta_o^2]/a_o^2$
K_{13}	$6x_\ell - 4a_o$	$[12\alpha^2 h_o^2 \beta_o(1 - \theta_4) + 6\alpha^3 h_o^3 \ell n(\theta_4) + 2x_\ell^3]/a_o^2$
K_{14}	$\beta_o(1 + \beta_o)$	$\beta_o(-1 + \beta_o)[\theta_4^2(a_o - \beta_o) + \beta_o]/a_o$
K_{15}	$1 - 2\beta_o$	$(1 - 2\beta_o)\theta_4 + \beta_o(-2 + 3\beta_o)(\theta_4 - 1)/a_o$
[5] K_{16}	$\ell n(1 - \phi)$	$\ell n(\theta_5) + [a_o - x_\ell + (1 - 3\beta_o)\ell n(\theta_4)]/a_o$
K_{17}	$a_o^2(-2 + a_o) + 2x_\ell^2(3 - 2x_\ell)$	$x_\ell^3(4 - 3x_\ell)/a_o$

[1] I_1: $D \leq (m - a)/\alpha$ (see fig. 1)

[2] I_2: $D > (m - a)/\alpha$

[3] $x_\ell = \beta_o - \alpha h_o$

[4] $\theta_4 = \alpha h_o/(\beta_o - a_o)$

[5] $\theta_5 = (1 - \phi)\theta_4$

U.S. GOVERNMENT PRINTING OFFICE 1984 [illegible]

2.3-12/84

END

FILMED

2-85

DTIC